

Development of an Intermodal Container Load Status and Security Monitoring System

**Roy McCann
MBTC 2084
June 2008**

DISCLAIMER

The contents of this report reflect the views of the authors, who are responsible for the facts and the accuracy of the information presented herein. This document is disseminated under the sponsorship of the Department of Transportation, University Transportation Centers Program, in the interest of information exchange. The U.S. Government assumes no liability for the contents or use thereof.

ABSTRACT

There is increasing concerns regarding national security risks associated with international freight and cargo shipments. The existing container/trailer security monitoring systems for transportation logistics use conventional methods and technologies such as video cameras, infrared sensors and ultrasonic proximity sensors (line of sight configuration). However high cost, failures owing to adverse weather conditions, inaccurate detection of cargo condition due to variable material/configurations encountered in freight transport are some of the reasons for the limited success of conventional monitoring systems. This research applies signal processing techniques to the analysis of acoustical responses which contributes toward the development of an intermodal container load status and security monitoring system. In this manner, the drawbacks of the existing conventional methods are reduced by incorporating the recent advances in radio frequency identification (RFID) technology and acoustical signature monitoring (ASM). Experimental results are given demonstrating that the concept of ASM is an effective technique for improved monitoring and load status assessment of intermodal containers and trailers.

TABLE OF CONTENTS

1. Introduction.....	1
1.1 Introduction: Problem Statement.....	1
1.1.1 Current technologies to monitor trailers/containers.....	1
1.2 Alternative proposal: Research Approach.....	6
1.3 Scope.....	6
1.4 Organization of this Report:	7
2. Methodology: Sound, reverberation and absorption properties.....	8
2.1 Sound:	8
2.2 Absorption and Reverberation.....	9
2.2.1 Absorption coefficient	10
2.2.2 Reflection coefficient.....	10
2.3 Absorptivity of different materials [7].....	10
2.4 Reverberation.....	17
2.5 Relevance of acoustics in this report	18
3. Methodolgy: Fourier transforms.....	20
3.1 Fourier transform.....	21
3.1.1 Continuous Fourier transform (CFT).....	21
3.1.2 Discrete Fourier transform (DFT)[8].....	22
3.2 Fast Fourier transform	25
3.2.1 Radix-2 FFT.....	26

4. Methodolgy: Short-term fourier transform and wavelet transform	31
4.1 Example showing Fourier transform of a uniform and nonuniform signal	32
4.2 Short term Fourier transform	36
4.3 Wavelet transform:	39
5. Findings: Data and data collection	40
5.1 Data collection:	40
5.2 Actual data	42
6. Analysis and Conclusions.....	47
6.1 Graphical results	47
6.2 Two and Three dimensional plots for the remaining conditions:	55
6.2.1 Analysis of 2D and 3D graphical results	63
6.3 Conclusion	67
6.4 Future work.....	69
APPENDIX A.....	71
A.1 Wavelet transforms	71
A.2 Continuous wavelet transform	72
A.3 Discrete wavelet transform	73
A.4 Decomposition filter	74
A.5 Applications of wavelet transform.....	77
APPENDIX B.....	80
Introduction.....	80
B.1 Sound pressure	80
B.2 Sound pressure level (SPL).....	80

B.3 Sound power.....	82
B.4 Sound power level.....	82
References.....	83

LIST OF FIGURES

Figure 1: Variation of sound pressure level with variation in absorptivity.	12
Figure 2: Absorptivity of different porous materials.	13
Figure 3: Absorptive characteristics of nonporous materials.	15
Figure 4: Time domain signal representing (3.7).	24
Figure 5: Fourier transform of the signal $x(t)$ showing the presence of frequencies at 10, 50, 100 and 200 Hz.	25
Figure 6: Butterfly diagram for 2-point DFT.	28
Figure 7: Butterfly diagram for an 8-point FFT.	30
Figure 8: Signal representing (4.1).	33
Figure 9: Fourier transform of the signal in (4.1).	33
Figure 10: Nonuniform signal with frequency varying from 100 Hz to 250 Hz.	34
Figure 11: Different representation of the nonuniform signal with frequencies from 100 Hz to 250 Hz.	35
Figure 12: Fourier transform of nonuniform signal with frequency 100 and 250 Hz 36	36
Figure 13: Example showing the calculation of STFT.	37
Figure 14: Calculation of STFT using sliding window method.	38
Figure 15: Figure showing the dimensions of the trailer/truck (side view and rear view) and positions of the mic and the acoustical excitation source (AES).	40
Figure 16: Echo sample for the case with truck/trailer empty, doors closed.	42
Figure 17: Echo sample for the case with truck/trailer empty doors open.	42
Figure 18: Echo sample for the case with trailer full doors closed.	43
Figure 19: Echo sample for the case with trailer full doors open.	43

Figure 20: Echo sample for the case with trailer one-third full doors closed.	44
Figure 21: Echo sample for the case with trailer one-third full doors open.	44
Figure 22: Echo sample for the case with trailer two-thirds full doors closed.	45
Figure 23: Echo sample for the case with trailer two-thirds full doors open.....	45
Figure 24: Echo sample for the case with truck empty door closed.	47
Figure 25: Echo sample for the case with trailer empty door open.	48
Figure 26: FFT, in logarithmic scale, of the time signals in Figure 24 and 25.....	49
Figure 27: FFT, in linear scale, of the time signals in Figure 24 and 25.....	49
Figure 28: Two-dimensional plot of STFT for the signal in Figure 24 (truck/trailer empty doors closed).	51
Figure 29: Two-dimensional plot of STFT for the signal in Figure 25 (truck/trailer empty doors open).....	51
Figure 30: Three-dimensional plot of STFT for the signal in Figure 24 (truck/trailer empty doors closed)	52
Figure 31: Three-dimensional plot of STFT for the signal in Figure 25 (truck/trailer empty doors open).....	52
Figure 32: Two dimensional plot for the case with truck one-third full doors closed.....	55
Figure 33: Two dimensional plot for the case with truck one-third full doors open.	55
Figure 34: Three dimensional plot for the case with truck one-third full doors closed....	56
Figure 35: Three dimensional plot for the case with truck one-third full doors open.	56
Figure 36: Two dimensional plot for the case with truck two-thirds full doors closed. ...	58
Figure 37: Two dimensional plot for the case with truck two-thirds full doors open.	58
Figure 38: Three dimensional plot for the case with truck two-thirds full doors closed. .	59

Figure 39: Three dimensional plot for the case with truck two-thirds full doors open. ...	59
Figure 40: Two dimensional plot for the case with truck full doors closed.	61
Figure 41: Two dimensional plot for the case with truck full doors open.	61
Figure 42: Three dimensional plot for the case with truck full doors closed.	62
Figure 43: Three dimensional plot for the case with truck full doors open.	62
Figure 44: Color-map-editor for 2D plot for the case truck empty and door closed	66
Figure 45: Color-map-editor for 3D plot for the case truck empty and door closed.	67
Figure 47: Continuous wavelet transform.	72
Figure 48: Corrupted sinusoidal signal of frequency 10 Hz.	75
Figure 49: Low frequency and high frequency components after 1 st stage filtering.	76
Figure 50: Low and High frequency components after second and third stage filtering..	77

1. INTRODUCTION

1.1 Introduction: Problem Statement

One of the most important means of transportation of goods is inter-modal freight containers and logistic carriers including truckload (TL) and less-than-truckload (LTL). Electronic monitoring of freight containers/trailers is essential and serves two objectives: ensuring the security of the container and streamlining of the supply chain.

1.1.1 Current technologies to monitor trailers/containers

The present security scenario in the world mandates that minimizing the opportunity to breach transport security systems with the intention of creating mayhem and destruction. Containers/trailers are one of the easiest targets in breaching the security because millions of containers travel around the world passing different hands from manufacturer to ports to marine vessels through sea lanes and finally to end users.. An estimated seven to nine million containers come to US ports every year. It is humanly impractical to physically check each and every container. Some of the traditional methods for container/trailer monitoring system involve the use of video cameras, ultrasonic proximity sensors, X-ray scanning. The use of video cameras in tractor trailers have disadvantages like distracting the driver which might lead to accidents, also, the cost factor is high. Ultrasonic proximity sensors also have few disadvantages due to the fact that ultrasonic waves are directional. The ultrasonic proximity sensors are placed at the front of the container/trailer to monitor the load status. The load in front of sensor can block the line of sight of the sensor and this makes the load at the other end of the trailer vulnerable for

theft and tampering. X-ray scanning method is costly and is performed only at ports where such facilities are available. After leaving the ports the containers are still susceptible to tampering during their journey between any two points and there is no way of knowing it if there is no effective monitoring techniques.

Different technologies are used to overcome these loopholes. The technologies currently being used are, Radio Frequency Identification (RFID), cellular and satellite communications, Global positioning system (GPS) and Wi-Fi. A brief description of these technologies is given below.

1.1.1.1 RFID

RFID is an acronym for Radio Frequency Identification. The present day RFIDs operate in the frequency range 50 kHz to 2.5 GHz. The complete RFID system consists of a tag and a reader. The tag consists of a microchip to store information related to a particular product and an antenna to transmit this information. Based on power source there are mainly two types of tags, active and passive. Based on range there are two types, short range and long range and based on memory attributes there are mainly two, read and read/write types. The active tags use battery to drive the microchip while the passive derives power from the RFID reader when it emits RF waves on the tag. For any meaningful communication to take place between the two, they should be tuned to the same frequency [1].

Passive tags are used in such cases where the items don't need high security and in short range operations. Active tags, because of their independent power supply, can have other security features like GPS system, temperature, pressure and humidity sensors. Some of the main advantages of RFID tags over bar code system are

- RFID does not operate on the line of sight principle for communication between the tag and the reader.
- RFID can store more information about a product than a bar code system.
- By improving supply chain, reducing labor costs and losses, RFIDs help to improve logistics, customer relationship management, manufacturing resource planning and enterprise resource planning by way of improving supply chain integrity, reducing labor costs and reducing losses.

For all the advantages the RFID technology has to offer, it has many issues which are affecting the implementation process. Research by some companies in this regard shows some of these issues:

- Type of tag and method of securing the tags on goods: Liquids like paint, oil absorb radio waves and hence difficulty in reading.
- Special software is needed to read the tags when they are moving on the conveyer so as to avoid multiple reading of the same tag or missing reading the tag.
- The present database management systems are suitable for barcode system and since RFID is different from bar code system, sufficient investment has to be made to come up with methods to integrate RFID into the present inventory and database systems.

- RFID stores much more information than the currently existing barcode systems. Movement of such large quantities of data over the network takes up considerable bandwidth of the network and its components.

1.1.1.2 GPS

A great deal of general information about GPS is available in the public domain and can be found on the internet as well. GPS is a satellite navigation system which helps in finding the time and location of an object or person in any part of the world. The system is funded and controlled by US government. It uses a little more than two dozen satellites. At any time four satellites are required to calculate the position (X, Y, Z coordinates) and time. GPS as applied to the container security system is helpful in such places where there are no cellular or satellite coverage to keep track of the container. It has been found that because of the way containers are stored, GPS signals are frequently blocked or reflected multiple number of times and this has constrained the use of GPS systems in container tracking technology. However, research is being done to overcome this problem of signal reception [2].

1.1.1.3 Satellite and cellular communication

Inside the geographical boundaries of a country, it is economical to use cellular networks and low earth orbit satellites to keep track of containers. Cellular messaging can be used to transfer data about the position and status of the container.

1.1.1.4 Wi-Fi

Wi-Fi stands for Wireless Fidelity (though some controversy still surrounds the usage of this name). Wi-Fi is a general term used to refer to any IEEE 802.11 network. A product that is Wi-Fi certified can communicate with an access point (communication hub) of any brand. Wi-Fi systems have intermediate ranges and can help locate assets in a yard. Wi-Fi enabled RFID readers can help in reading RFID tags of the containers for data collection and verification purposes.

RFID technology integrated with GPS, satellite and cellular communication systems, Wi-Fi systems help in tracking the container position and load status. From the security point of view, the inherent assumption is that tampering with load involves directly tampering with RFID tags/seals and this information will then be conveyed through GPS or satellite and cellular communication systems or Wi-Fi systems. However, in the event of a container/trailer breach there is a possibility that an RFID tag could be removed from the packaging material without damaging it and left behind while the asset is removed. Such a security breach will not involve direct tampering of the RFID tag and hence there will not be any alerts. Also, the existing technology detects such a security breach if it happens through the doors, but if the container/trailer is cut open on the top or sides, then these existing devices are not activated. To fill in such a gap in the security system we can use acoustical signature monitoring (ASM) method. The principle on which this method works is given in the next section.

1.2 Alternative proposal: Approach of Research

ASM is based on the principle that the acoustical response of a structure, such as the interior of an inter-modal container, to a short duration broad frequency excitation will have a characteristic echo depending upon the condition (container completely shut/open) and the load level (empty/full etc). In addition, recent research has developed methods to discern frequencies of interest from background noise that would be encountered during rail or truck movement. ASM provides an independent monitoring means to RFID technology. As described in the previous section, if an attempt is made to breach the security, the ASM technique would detect either the change in acoustic properties due to the breach itself, or the removal of the asset packaging due to the change in the acoustical signature of the container/trailer at the time of stealing.

1.3 Scope

This report demonstrates that the concept of ASM is a more effective technique than the currently available methods to monitor the load status of intermodal container/trailers. The ASM techniques will build upon what has been introduced in automotive applications for diagnostic monitoring of internal combustion engines and passenger compartment noise cancellation [3]-[4]. The principle is that a structure such as an inter-modal container can be excited with a broadband acoustical impulse, and the time-varying frequency content of the echo is indicative of the load status (door open/shut, empty, partially loaded, full, container breach from hole cutting, etc.). This method has

been shown to reject ambient noise conditions such as wind noise and road vibration. In addition, the system can be configured to self-diagnose for failures and tampering.

1.4 Organization of this Report:

Chapter 2 describes the acoustical characteristics for different materials. Chapter 3 explains Fourier transform (FT) and fast Fourier transform [FFT]. Chapter 4 deals with short-term Fourier transform (STFT). Chapter 5 deals with data collection methods, factors considered for data collection and the acquired data. Chapter 6 deals with the analysis of results for validating ASM and conclusion.

2. METHODOLOGY: SOUND, REVERBERATION AND ABSORPTION PROPERTIES

This report concentrates on acoustical signature monitoring (ASM) and it is necessary to look into some of the aspects of acoustics, its properties, and the parameters that have to be taken into account in the implementation of ASM.

One way of defining acoustics is the scientific study of sound waves, including its generation, transmission and reverberations. The rest of this chapter deals with sound waves, reverberation, and absorption properties of materials. Much of the information used in this chapter was collected from the books: ‘Applied Acoustics ’ by Porges G [5], ‘Fundamentals of Noise and Vibration Analysis for Engineers’ by Michael Norton [6] and Denis Karczub, and ‘Acoustic Design and Noise Control’ by Michael Rettinger [7].

2.1 Sound:

Sound can be described as the propagation of disturbance through a medium in the form of waves. If we consider the medium as air, then the disturbance of particles (that make up the air as a medium) can be considered as the change in the energy of the particles and this change in energy is transferred to the neighboring particles and this way the sound waves propagate. In other words, we can consider sound waves to be a variation of pressure that propagates through the medium. Sound waves are longitudinal waves, meaning, that the direction of the movement of the particles in the medium and that of the wave is one and the same. When sound waves propagate through a medium they create

what are called compressions and rarefactions. Compressions are areas where particles of the medium are very close to each other and rarefactions are areas where the particles are far apart. The distance a sound wave can propagate depends on various factors like frequency of the wave, density of the media, elasticity and inertia of the particles of the media.

If we consider the wavelength ' λ ' as the distance traveled by a wave in one period ' T ' at a speed of ' c ', then we can write the following equation.

$$c = \lambda / T \quad (2.1)$$

Since, frequency ' f ' is the inverse of the period, we can rewrite (2.1) as

$$c = \lambda f \quad (2.2)$$

One of the most commonly used medium for sound wave propagation is air. The velocity of sound in air is found to be independent of pressure but is proportional to the square root of temperature [5].

2.2 Absorption and Reverberation

Absorption in the present context refers to the amount of sound energy that is absorbed. Reverberation means repeated reflections of sound waves. The audibility of sound inside a room or enclosure depends on factors like the area of the room and its design, the materials used inside the room, on walls, flooring (hard wooden floor or carpet flooring), number of windows and the number of people inside the room. Each of these factors absorbs or reflects the sound waves to a varying degree.

2.2.1 Absorption coefficient

Absorption coefficient, sometimes also referred to as absorptivity, is defined as the ratio of absorbed sound energy to the incident energy. Absorption coefficient depends on the angle of incidence, frequency and the way material is used [5].

2.2.2 Reflection coefficient

Reflection coefficient is defined as the ratio of reflected sound energy to the incident energy [5]. Since in practice the amount of reflected energy is always less than the incident energy, this ratio is always less than 1. We can now mathematically define absorption coefficient as 1 minus reflection coefficient. If we consider the absorption coefficient to be ‘ α ’, then reflection coefficient can be written [5] as,

$$\beta = 1 - \alpha \quad (2.3).$$

Apart from absorption and reflection, we have to consider the amount of energy, however small, transmitted through the walls. If this coefficient is represented by the letter ‘ τ ’, then we can write the following equation,

$$\alpha + \beta + \tau = 1 \quad (2.4).$$

2.3 Absorptivity of different materials [7]

The total absorption coefficient of an enclosure ‘ α_T ’ is usually referred to as Sabine absorption coefficient and this is used in calculating the reverberation time [6]. The amount of heat generated due to sound energy dissipation is very small and hence

logarithmic units called ‘decibels’ or dB [13] is widely used to measure the sound pressure level (SPL) (more information about sound power, sound power level, sound pressure, sound pressure level and the units used to measure these can be found in appendix B).

The Figures 1(a)-1(c) on page 12 illustrates the variation in reflected energy (sound pressure level) with the variation in absorptivity. If we consider the incident wave to have SPL of 70dB, depending on the absorptivity of the material, the SPL of the reflected wave will have different values. If the absorptivity of the material is high, then the SPL of the reflected wave will be less. If the absorptivity of the material is low, then the SPL of the reflected wave will be more.

Figure 1(a) illustrates the case where absorptivity is less (50%) and the SPL of the reflected wave (67dB) among the three cases shown. The illustration in Figures 1(b) and 1(c) shows examples where the material has high absorptivity and hence has low SPL of reflected wave, 60dB and 50dB. The reduction in the SPL is given by the formula [7]

$$\text{Sound pressure level reduction} = 10 \log(1 - \alpha) \text{dB} \quad (2.5).$$

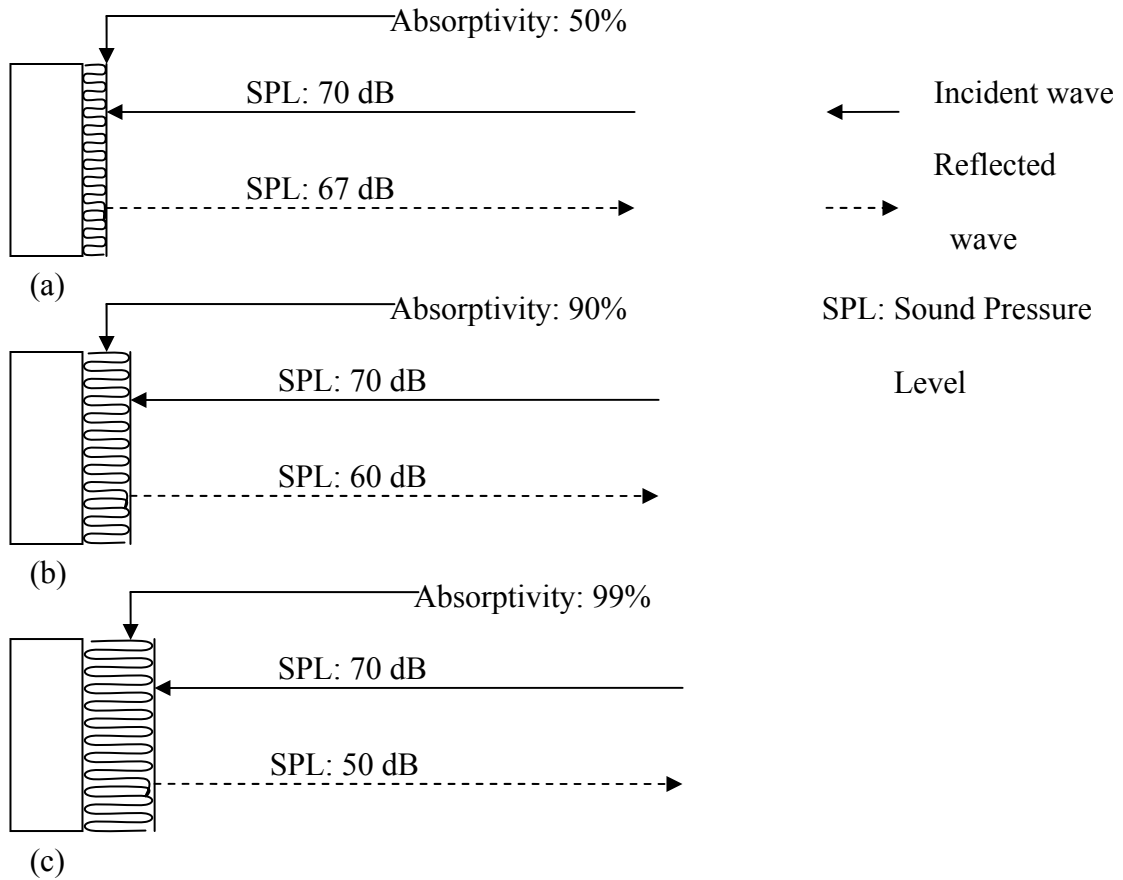


Figure 1: Variation of sound pressure level with variation in absorptivity.

Some of the factors that determine the absorptive property of a material are softness, hardness, thickness and porosity which are a measure of how densely a material is packed. It has been found that soft materials like cotton, mineral wool etc. are low frequency absorbents compared to the stiff materials like wood, ceramic tiles etc. Also, it has been found that, to a limit, thicker materials are more absorptive for low frequencies [7]. The Figure 2 [7] (page 13), shows the absorptive characteristics of different porous materials.

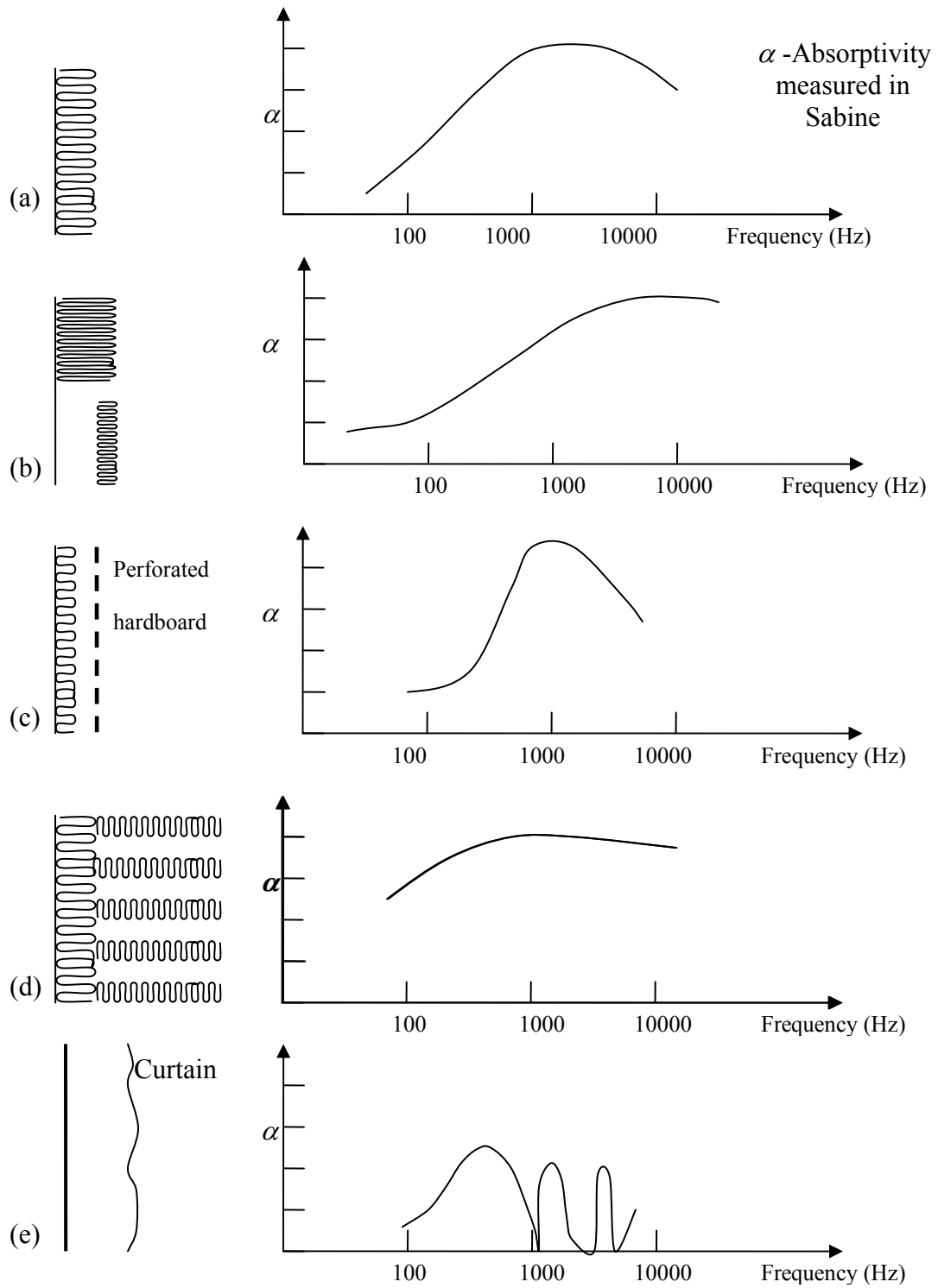


Figure 2: Absorptivity of different porous materials.

Figure 2(a) is an example of commercially available acoustic tile with thickness ranging from $\frac{1}{2}$ to 1 inch. As thickness increases the low frequency absorption capacity increases.

Figure 2(b) is an example for thicker, softer and more porous material like Owens-Corning PF fiberglass board no.615, with 3 inch thickness or the same material with 1 inch thickness separated from hard backing by 2 inches. The frequency response shows that such materials are high frequency absorbers.

Figure 2(c) is an example for a soft material sandwiched between hard wall and perforated hardboard. This type is usually mid frequency absorbers. In other words high frequency and low frequency are least absorbed compared to mid frequencies.

Figure 2(d) is an example of a series of deep, sound absorbent panels. In this case the reflections from boundary surfaces are negligible.

Figure 2(e) is an example of a curtain in front of a hard wall. In such cases, it has been found that maximum sound will be absorbed if the distance between the wall and the curtain is equal to quarter of a wavelength or an odd multiple thereof and minimum sound will be absorbed when the distance between the wall and curtain is one half the wavelength or an even multiple thereof. The number of folds and deep furling increases the high frequency absorptivity. Figure 3 [7] on page 15 and 16 shows the absorptive characteristics of nonporous materials.

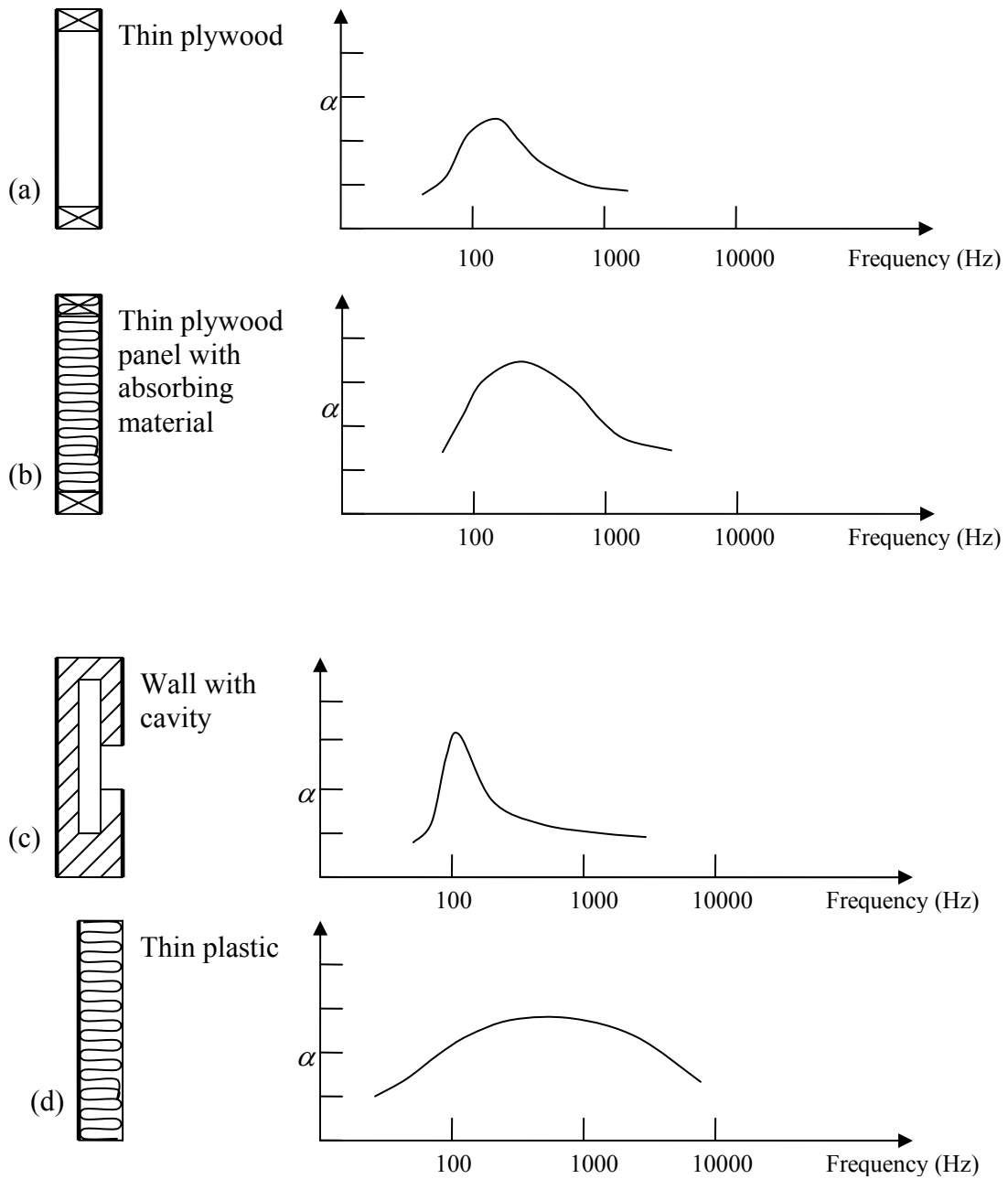


Figure 3: Absorptive characteristics of nonporous materials.

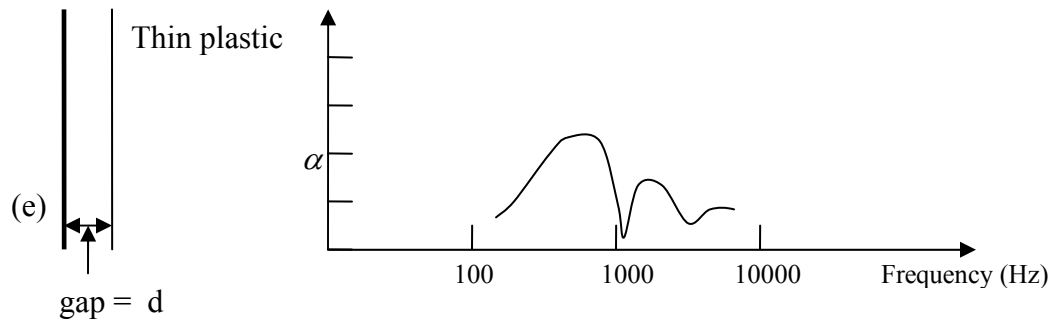


Figure 3 (contd): Absorptive characteristics of nonporous materials.

In Figure 3(a), we have an example where a thin plywood panel is clamped against studs, creating a gap between the hard wall and the plywood. This distance between the wall and plywood panel determines the resonance frequency of the panel. If the distance is more, then the resonant frequency will be lowered and if the distance is less, then the resonant frequency will be raised.

In Figure 3(b), we have an example similar to the set up in Figure 3(a), the difference however is that the air gap is filled with a sound absorbent material whose effect can be clearly understood by observing the graph of absorptivity Vs frequency in Figure 3(b). The difference in graphs between Figure 3(a) and Figure 3(b) is that in Figure 3(b) the frequency absorbing range is broadened because of the presence of sound absorbent material.

In Figure 3(c), we have an example which illustrates the absorptive nature of a wall that has hollow cavities. The cavities are filled with materials like fiber glass, sponge etc. Such an arrangement has high absorptiveness at frequencies between 100 Hz and 250 Hz.

In Figure 3(d), we have an arrangement where soft sound absorbing material like fiber glass, sponge rubber, etc is placed between wall and a thin plastic sheet. If the plastic sheet is very thin of the order of 0.01 g/ft^2 we will get absorptive behavior shown in the figure. If the material is thicker, then, the absorption characteristics will be similar to what is shown in Figure 3(a) and (b).

In Figure 3(e), the arrangement is similar to that in Figure 3(d), but there is no sound absorbent material. The absorption characteristics show that there will be lot of reflections because of the nonabsorptive nature of the plastic sheet.

2.4 Reverberation

As mentioned in section 2.2, reverberation is a phenomenon where there will be repeated reflections of sound waves. Most enclosed spaces and partially enclosed spaces that are not covered by sound absorbing materials exhibit reverberations. The frequency characteristics of reverberations in case of completely enclosed space is different from the frequency characteristics of partially enclosed spaces and spaces that has sound absorbing material.

For large music halls, some amount of reverberation is desired to enhance the quality of interpretation of music. In contrast, class rooms will have low or negligible amount of reverberations. Reverberation can be reduced using more sound absorbing materials like fiber glass, sponge rubber, styrofoam etc. Using these materials on the boundaries of the room will help in reducing reverberations by absorbing most of the incident energy and

reflecting a small amount of incident energy. This reflected energy in turn will be partially absorbed and partially reflected. After many such absorptions and reflections the amplitude of the reflected sound becomes negligible.

Many pioneers in the field of acoustics have come up with mathematical equations to calculate the reverberation time by considering the absorptive or reflection coefficient of the materials inside the room and the areas of such materials. However, those topics are beyond the scope of this chapter.

2.5 Relevance of acoustics in this report

As mentioned at the beginning of the chapter, this report concentrates on ASM. The way the principle of ASM works can be summed up as given in the next two paragraphs.

A container/trailer is made of metal and the inside of the container will also be metal in many cases. In some cases the interior could be plywood or other soft material placed against hard metal outer walls. The presence of metal or soft material as interior gives different kind of reverberations. The graph of absorptivity Vs frequency will be different depending on the type of material in the interior of the container. The presence or absence of load further determines the unique absorptive or reflective characteristics.

A fully loaded container with metal interior gives a different frequency response compared to a fully loaded container with soft material as interior. If the door is open or any part of the container is cut open the reverberation characteristics will be different and

thus any attempts to steal the load can be detected. A similar observation can be made for different load status or conditions like, container empty and door shut, container empty and door open, container full and door shut, container full and door open or partially open. Each of these conditions gives different frequency characteristics and we can use this data to determine the load status of the container.

3. METHODOLOGY: FOURIER TRANSFORMS

“Signals are described and represented in different ways. They reflect a physical phenomenon that conveys information. The information inside the signal may be contained in a pattern of some variations. Mathematically a signal is defined as a function of one or more independent variables like time, pressure, temperature etc. When the independent variable is time, the signal is referred to as time domain signal and it may represent current, voltage or any other factor like pressure as in case of geophysics” [16].

Time domain signals can be broadly classified as continuous-time signals (also referred as analog signals) and discrete-time signals. In case of continuous time signals the independent variable is continuous and the signal is defined for a continuum of values. A continuous time domain signal is represented as $x(t)$ where ‘t’ represents the continuous time. In case of discrete time signals the independent variable takes only discrete values and hence the signal is defined only at discrete times, essentially it is a sequence of samples represented as numbers. A discrete time domain signal is represented as $x[n]$, ‘n’ represents discrete time index.

Signal processing may be considered as a process or technique that deals with the representation, transformation, manipulation of signals and the information they contain. Processing of continuous time signals is generally referred to as continuous time signal processing or analog signal processing. Processing of discrete time signals involves processing of a sequence of numbers. One of the main uses of signal processing is to extract the frequency content of the signal for the purpose of signal analysis, synthesis,

and noise removal. A wide variety of techniques/procedures are available for this purpose, like, Fourier transforms, short-term Fourier transform, Hilbert transforms, Wavelet transforms, Wigner distribution, the Radon transform. This chapter will focus on the methods of frequency extraction using Fourier transforms and chapter 4 will focus on short-term Fourier transform.

The approach used to explain the concepts of Fourier transform in this chapter owes reference to the book, ‘Understanding Digital Signal Processing’, 2nd edition by Richard G. Lyons [8] where the author has explained about digital signal processing in a very simple, easily understandable way.

3.1 Fourier transform

Fourier transform is a mathematical approach to determine the frequency content of a signal. Fourier transform when applied to continuous time signals or analog signals is usually referred to as continuous Fourier transform.

3.1.1 Continuous Fourier transform (CFT)

The continuous Fourier transform is represented mathematically as

$$X(f) = \int_{-\infty}^{\infty} x(t)e^{-j2\pi(ft)} dt \quad (3.1),$$

where: $X(f)$ is the continuous Fourier transform, and it is a frequency domain function

$x(t)$ is the continuous time domain signal

f is the frequency

and t is time

The meaning of (3.1) is explained below.

The signal $x(t)$ is multiplied by an exponential term of some frequency ' f ' and then integrated from $-\infty$ to $+\infty$ and in practice this phrase "...integrated from $-\infty$ to $+\infty$..." means integrating over the entire length of the signal. Using Euler's relationship the exponential term can also be written as $\cos(2\pi ft) + j \sin(2\pi ft)$, this means that (3.1) can now be interpreted as $x(t)$ being multiplied by a complex sinusoidal signal of frequency ' f ' and then integrated over the entire length of the signal. If the result of integration is a large number then it shows that the correlation between $x(t)$ and the complex sinusoidal signal of frequency ' f ', is high. This also shows that the signal $x(t)$ has a major component of frequency ' f '. If the result of integration is a low value then it shows that the particular frequency is not a major component of the signal. Equation (3.1) is evaluated for different values of ' f ' and the corresponding values of $X(f)$ are calculated to find out all the frequency components in $x(t)$.

3.1.2 Discrete Fourier transform (DFT)[8]

Discrete Fourier transform is the discrete analogue of CFT. DFT is represented by the mathematical equation

$$X(m) = \sum_{n=0}^{N-1} x(n) e^{-j2\pi mn / N} \quad (3.2)$$

where:

$X(m)$ = the m^{th} DFT output component, i.e. $X(0)$, $X(1)$, $X(2)$ etc

m = the index of the DFT output in the frequency domain

Range of ' m ' = 0, 1, 2, 3,N-1

$x(n)$ = the sequence of input samples, $x(0)$, $x(1)$, $x(2)$ etc

n = the time domain index of the input samples, $n = 0, 1, 2, 3, \dots, N-1$

j = $\sqrt{-1}$

N = the number of samples of the input sequence and the number of frequency points in the DFT output.

If ' f_s ' is the sampling rate of a continuous time signal, then the frequency resolution is directly proportional to this sampling frequency and inversely proportional to the number of DFT points ' N ' and is given by the equation

$$f(m) = \frac{mf_s}{N} \quad (3.3)$$

Consider (3.2), using Euler's relationship the exponential term can be represented as $\cos(2\pi m / N) + j \sin(2\pi m / N)$. This means that $X(m)$ can have real and imaginary parts

$$X(m) = X_{real}(m) + jX_{imag}(m) \quad (3.4)$$

Having real and imaginary parts in the (3.4) allows us to conclude that $X(m)$ has a magnitude of $X_{mag}(m)$ and a phase angle of $X_{\phi}(m)$.

The magnitude of $X(m)$ is,

$$X_{mag}(m) = \sqrt{X_{real}(m)^2 + X_{imag}(m)^2} \quad (3.5)$$

and the phase angle of $X(m)$ is,

$$X_{\phi}(m) = \tan^{-1}\left(\frac{X_{imag}(m)}{X_{real}(m)}\right) \quad (3.6)$$

The way Fourier transform works can be shown using a pictorial example. Consider a continuous time signal that is made up of 4 sinusoids having frequencies 10, 50, 100 and 200 Hz i.e.

$$x(t) = \cos(2\pi 10t) + \cos(2\pi 50t) + \cos(2\pi 100t) + \cos(2\pi 200t) \quad (3.7)$$

In time domain this signal is as shown in Figure 4.

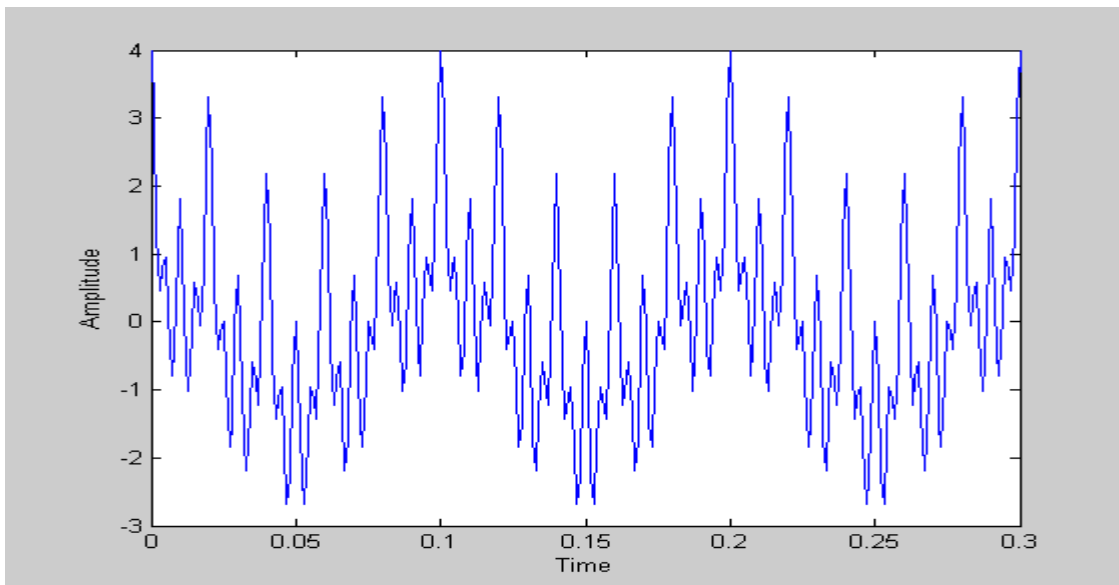


Figure 4: Time domain signal representing (3.7).

The Fourier transform of this signal shows the presence of frequencies at 10, 50, 100 and 200 Hz.

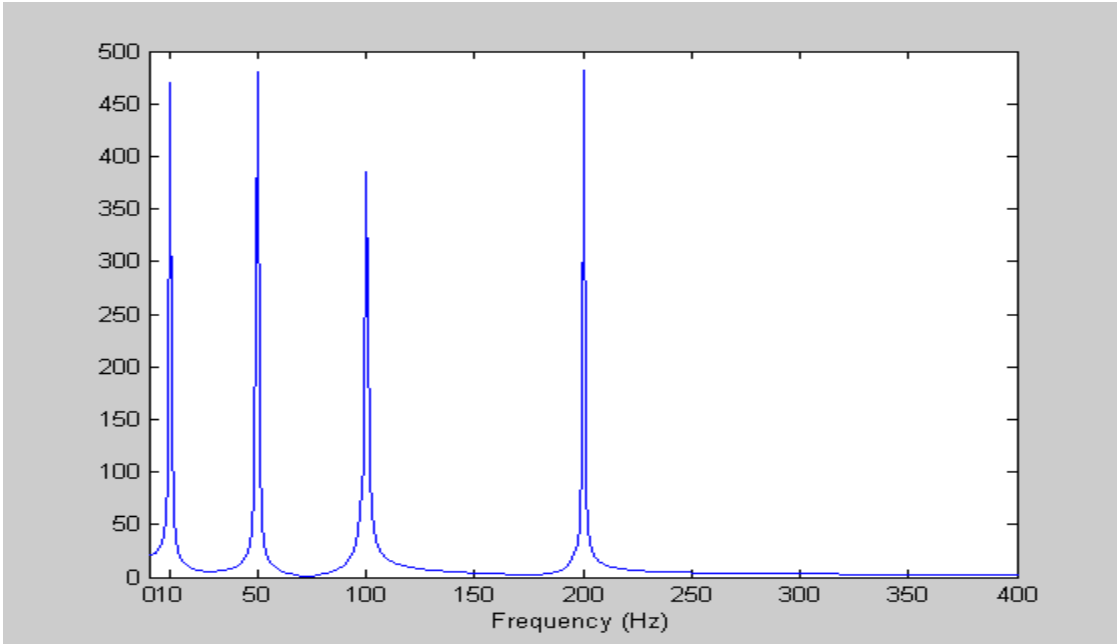


Figure 5: Fourier transform of the signal $x(t)$ showing the presence of frequencies at 10, 50, 100 and 200 Hz.

The Figures 4 and 5 were obtained using MATLAB, a software for technical computing and model based design [9].

3.2 Fast Fourier transform

Despite the fact that DFT is a direct mathematical procedure to determine the frequency content of a time domain signal, it has drawbacks when it comes to practical usage. As we increase the number of points in the DFT the necessary mathematical calculations become intense. Also there is a lot of redundancy associated with DFT. To overcome this problem a new algorithm was developed and it is called fast Fourier transform (FFT) [10]. The popular FFT algorithm is the radix-2 FFT and this is considered a very efficient

process for performing DFTs, however the DFT size should be an integral power of two, that is, the number of points in the transform should be $N=2^k$, where k is a positive integer. One of the main reasons for the efficiency and popularity of radix-2 FFT is the reduced number of calculations and thus reducing redundancies compared to DFT calculations.

Consider (3.2), which is the mathematical definition of DFT, here the number of complex multiplications necessary for an N point DFT is N^2 and the number of complex additions required is $N^2 - N$. Compared to this, the number of computations required by an N point radix-2 FFT is found to be approximately, $\frac{N}{2} \log_2 N$ [8] and this is a considerable reduction from the N^2 complex multiplications and $N^2 - N$ complex additions required by DFT (3.2).

3.2.1 Radix-2 FFT

This section deals with the structure (butterfly diagram) and operations of radix-2 FFT. Consider the DFT equation ((3.2) has been reproduced here for reference)

$$X(m) = \sum_{n=0}^{N-1} x(n) e^{-j2\pi mn/N}$$

Let $W_N = e^{-j2\pi/N}$, the W_N term is called *twiddle factor* and it exhibits periodicity and symmetry.

Periodicity: $W^{m+N} = W^m$

Symmetry: $W^{m+N/2} = -W^m$

Because of this symmetry and periodicity we have fewer computations in FFT compared to DFT. We can divide the summation in DFT equation into two terms with even and odd indices. The resulting equation will be

$$X(m) = \sum_{n=0}^{(N/2)-1} x(2n)e^{-j2\pi(2nm)/N} + \sum_{n=0}^{(N/2)-1} x(2n+1)e^{-j2\pi((2n+1)m)/N} \quad (3.8)$$

(3.8) can be reduced to

$$X(m) = \sum_{n=0}^{(N/2)-1} x(2n)W_N^{2(nm)} + W_N^m \sum_{n=0}^{(N/2)-1} x(2n+1)W_N^{2(nm)} \quad (3.9)$$

In the above equation each of the summation terms can be further split into even and odd indexed terms and this division continues till each of the summation term is left with just two terms at which point we have each summation representing a single 2-point DFT. The complete derivation of radix-2 FFT algorithm is considered beyond the scope of this chapter. Complete derivation of radix-2 FFT algorithm can be found in many digital signal processing books [8]. However the final equations can be represented as

$$X(m) = \sum_{n=0}^{(N/2)-1} x(2n)W_{N/2}^{nm} + W_N^m \sum_{n=0}^{(N/2)-1} x(2n+1)W_{N/2}^{nm} \quad (3.10)$$

and

$$X(m + N/2) = \sum_{n=0}^{(N/2)-1} x(2n)W_{N/2}^{nm} - W_N^m \sum_{n=0}^{(N/2)-1} x(2n+1)W_{N/2}^{nm} \quad (3.11)$$

The above two equations can be represented in simple terms as

$X(m) = R(m) + W_N^m I(m)$, and $X(m + N/2) = R(m) - W_N^m I(m)$. A single 2-point DFT can be represented using a diagram called butterfly diagram as shown Figure 6.

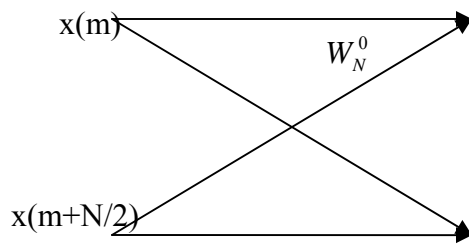


Figure 6: Butterfly diagram for 2-point DFT.

An example of 8 point FFT with complete butterfly diagram is shown in the Figure 7 (page 30). This diagram is also referred to as *decimation-in-time* FFT. Decimation-in-time refers to the division of DFT equation into odd and even indices in time domain. The effect of this decimation in time domain is the scrambled order of the inputs and this scrambled input is referred to as *bit reversal*. Also each FFT term is complex and the magnitude and phase can be found similar to DFT using (3.5) and (3.6). Table 3.1 shows bit reversal for an 8 point FFT.

Table 3.1: Input bit reversal for an 8-point FFT

FFT Index n in decimal	Index n in Binary	Bit Reversal of index n	Bit reversed order of n in decimal
0	000	000	0
1	001	100	4
2	010	010	2
3	011	110	6
4	100	001	1
5	101	101	5
6	110	011	3
7	111	111	7

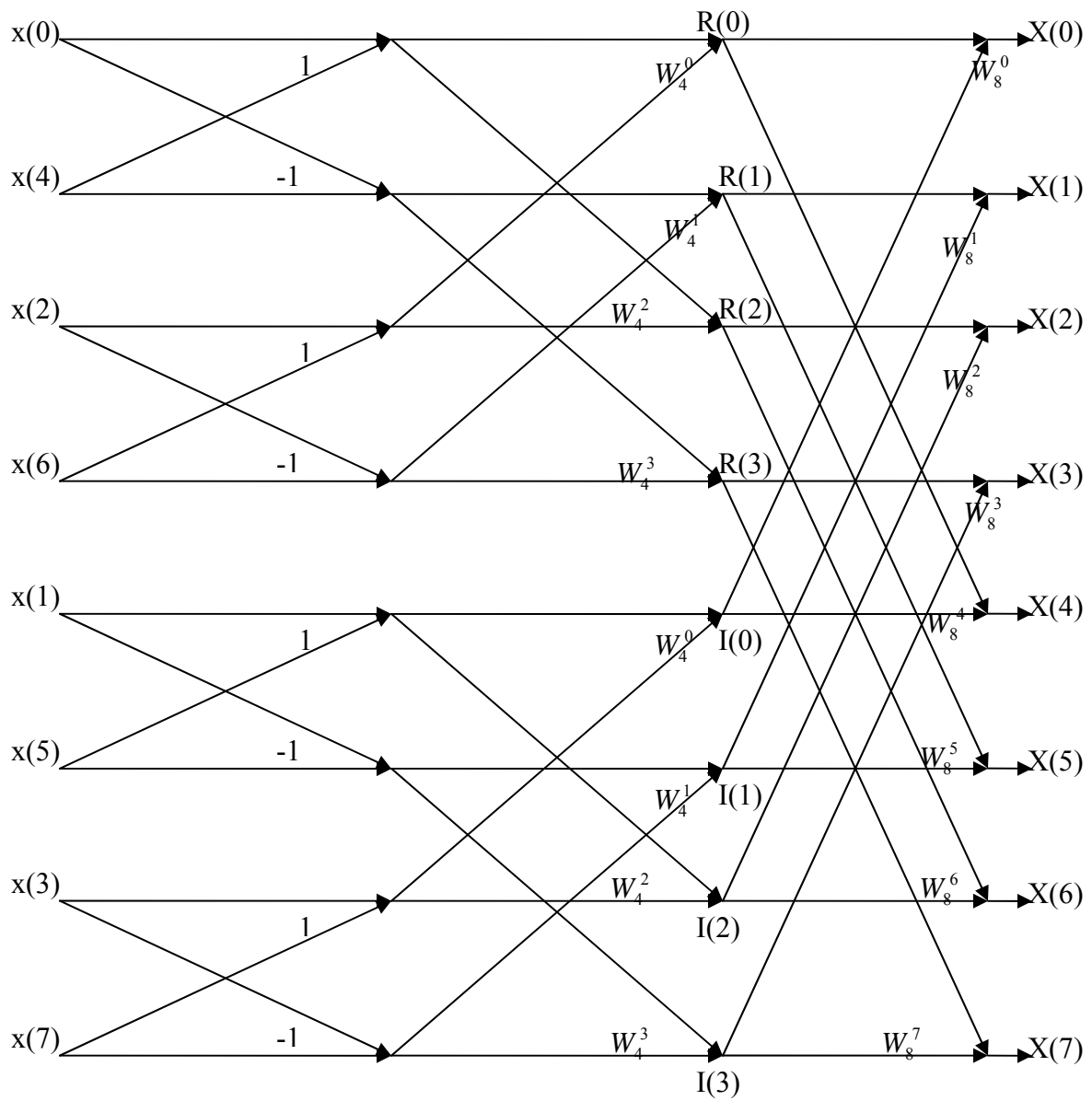


Figure 7: Butterfly diagram for an 8-point FFT.

4. METHODOLOGY: SHORT-TERM FOURIER TRANSFORM AND WAVELET TRANSFORM

Short-term Fourier transform (STFT) and Wavelet transforms are mathematical procedures for analysis, synthesis, noise removal and for other signal processing related functions. Like Fourier transform, both of them can be used to find the frequency content of the signal. However the difference is, STFT and wavelet transform give both time and frequency information about the signal, while the Fourier transform gives only frequency information. The usefulness of both time and frequency information of the signal depends on the application and also the type of signal, i.e., if the signal is uniform or nonuniform. In this report uniform signals refer to signals which have all the frequency components at all times and nonuniform signals refer to signals which have different frequency components at different times. The approach used to explain STFT in this chapter follows the approach used by Dr. Robi Polikar, Rowan Univeristy, for his course titled Theory and Engineering Applications of Wavelets [11] (information about this course is given in the reference section).

To understand the concept of STFT and wavelet transforms, it is important to understand the importance of time-frequency information in a time domain signal. The time-frequency information, in short, tells us what frequency components exist at what time. This is very useful in the analysis of nonuniform signals. Fourier transform helps in calculating only the frequency information about a time domain signal, it doesn't matter at what point of time in the signal that particular frequency appears and this is explained with an example in section 4.1. Though STFT and wavelet transform calculate both

frequency and time information of a time domain signal, one of the main differences between the two, is in the resolution of the information. Wavelet transform has a better resolution compared to STFT.

4.1 Example showing Fourier transform of a uniform and nonuniform signal

The example given in this section shows what Fourier transform can find and what it cannot find when applied to uniform and nonuniform signals [11]. This concept can be made clear from the following example. Consider the signal

$$x(t) = \sin(2\pi 100t) + \sin(2\pi 250t) \quad (4.1).$$

$x(t)$ in (4.1) is a uniform signal because the two frequencies 100Hz, 250Hz do not change in time and are present in the signal at all times. The signal is plotted in time domain and frequency domain as shown in Figure 8 (page 32) and Figure 9 (page 33) respectively.

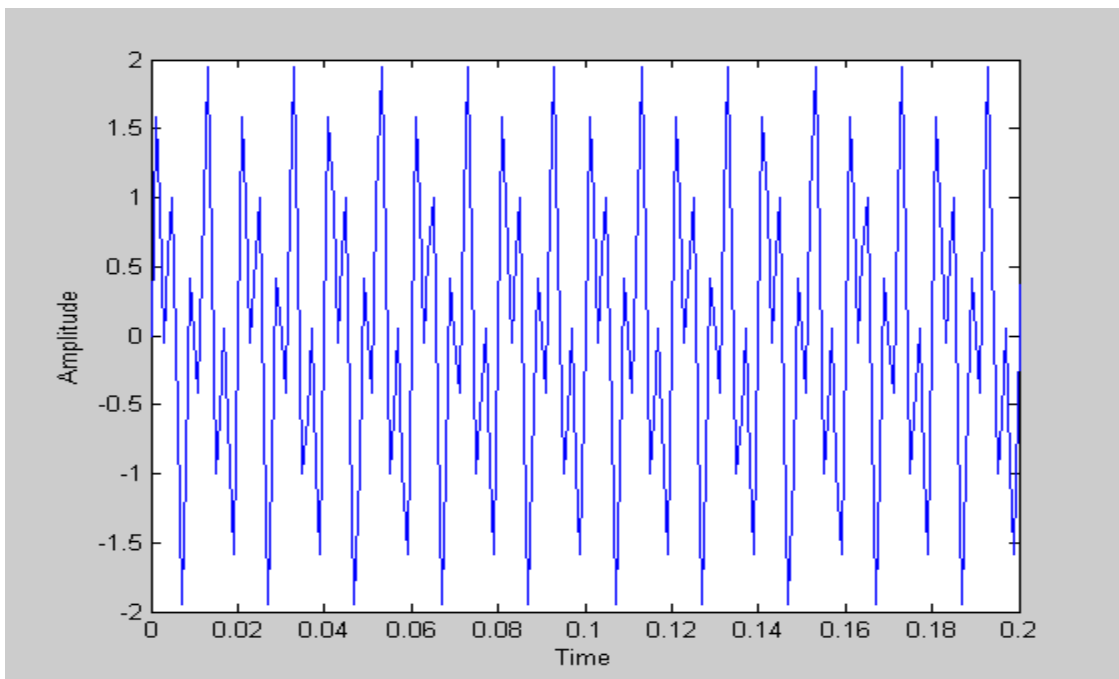


Figure 8: Signal representing (4.1).

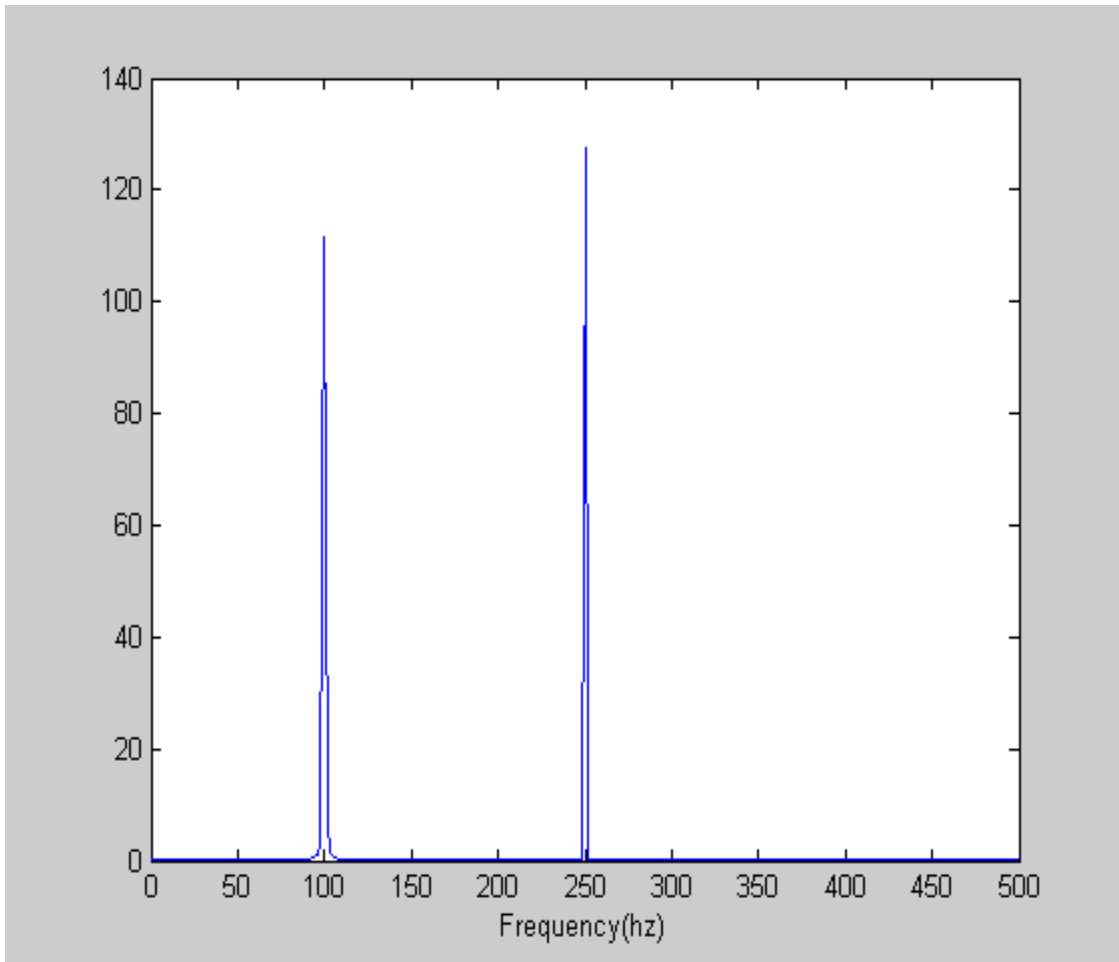


Figure 9: Fourier transform of the signal in (4.1).

Now consider a nonuniform signal that has the same frequencies 100 Hz and 250 Hz (as in the previous example) shown in the Figure 10 on page 34. The nonuniform signal in Figure 10 has 100 Hz from 0 to 0.2 seconds and 250 Hz from 0.2 seconds onwards.

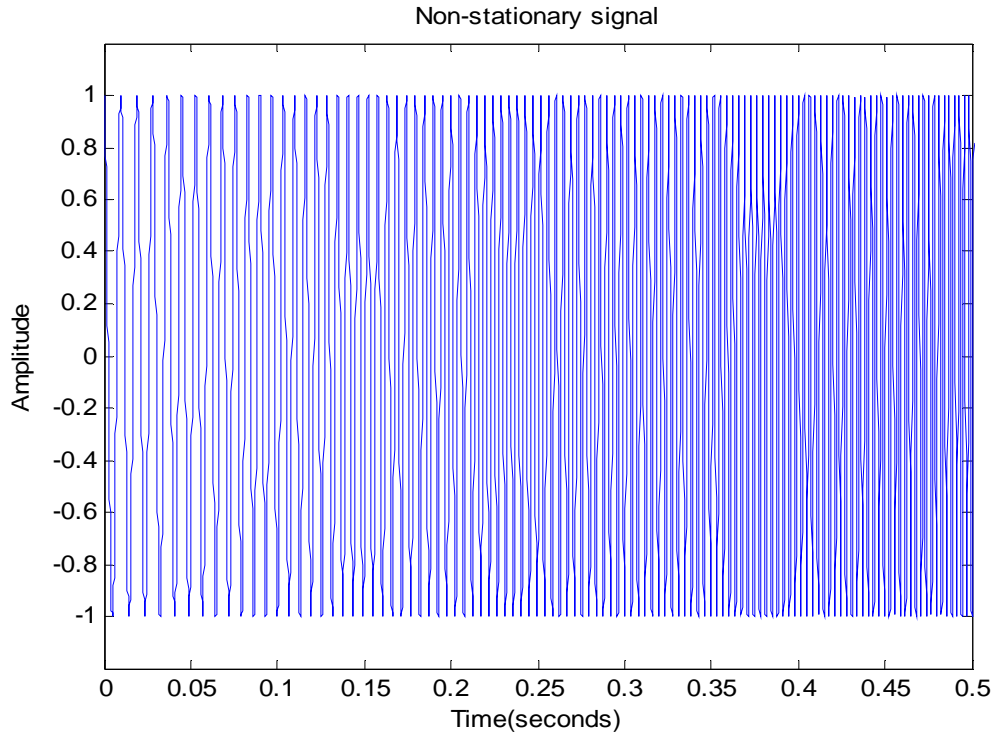


Figure 10: Nonuniform signal with frequency varying from 100 Hz to 250 Hz.

A nonuniform signal with frequencies as in Figure 10 i.e. 100 and 250Hz can also be represented as shown in Figure 11 on page 35. The difference between the two figures is that in Fig 11, the signal starts with 250Hz and stays on with that frequency until 0.3 seconds and from 0.3 seconds the frequency decreases to 100Hz.

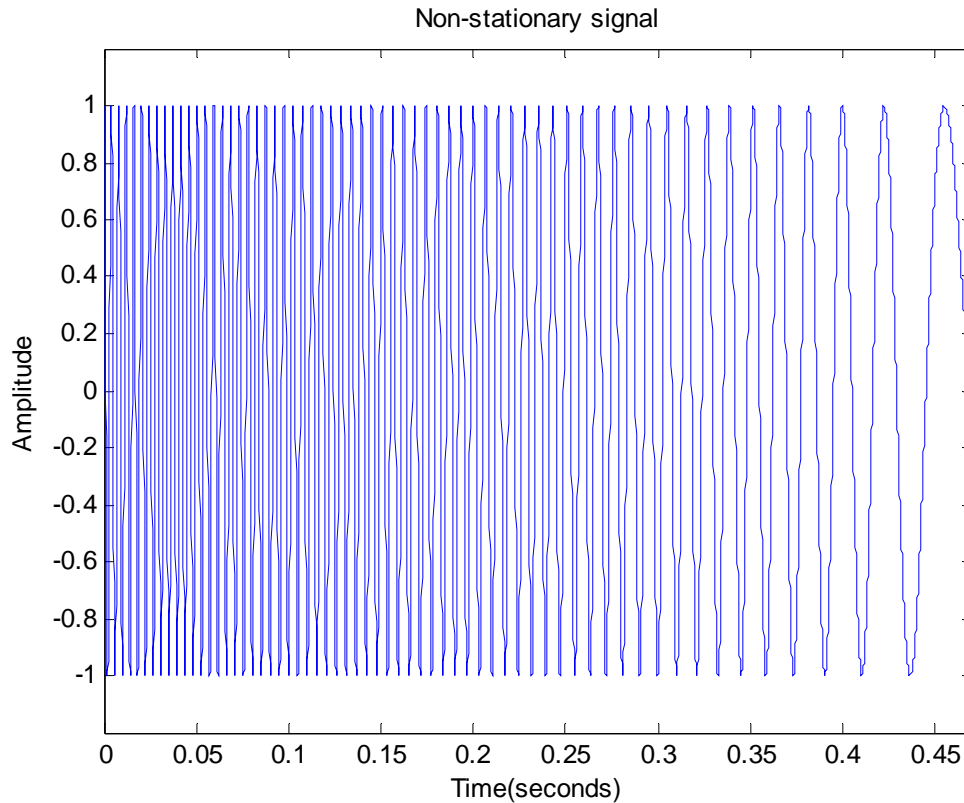


Figure 11: Different representation of the nonuniform signal with frequencies from 100 Hz to 250 Hz.

In the above two nonuniform signals the frequencies change with time and this aspect is different from a uniform signal shown in Figure 8 where all the frequencies exist at all the times.

The Fourier transform of the nonuniform signals mentioned in Figure 10 and Figure 11 is shown in Figure 12. The Fourier transform just shows the frequency content at 100Hz and 250Hz and does not provide information about the time factor. In some applications we need both the time information as well as frequency information. In such cases

Fourier transforms will not be useful. The Fourier transform does not tell at what time the frequencies occur in the signal. If we are only interested in the frequency content of the signal and not in its time information then we can still use Fourier transform for nonuniform signals.

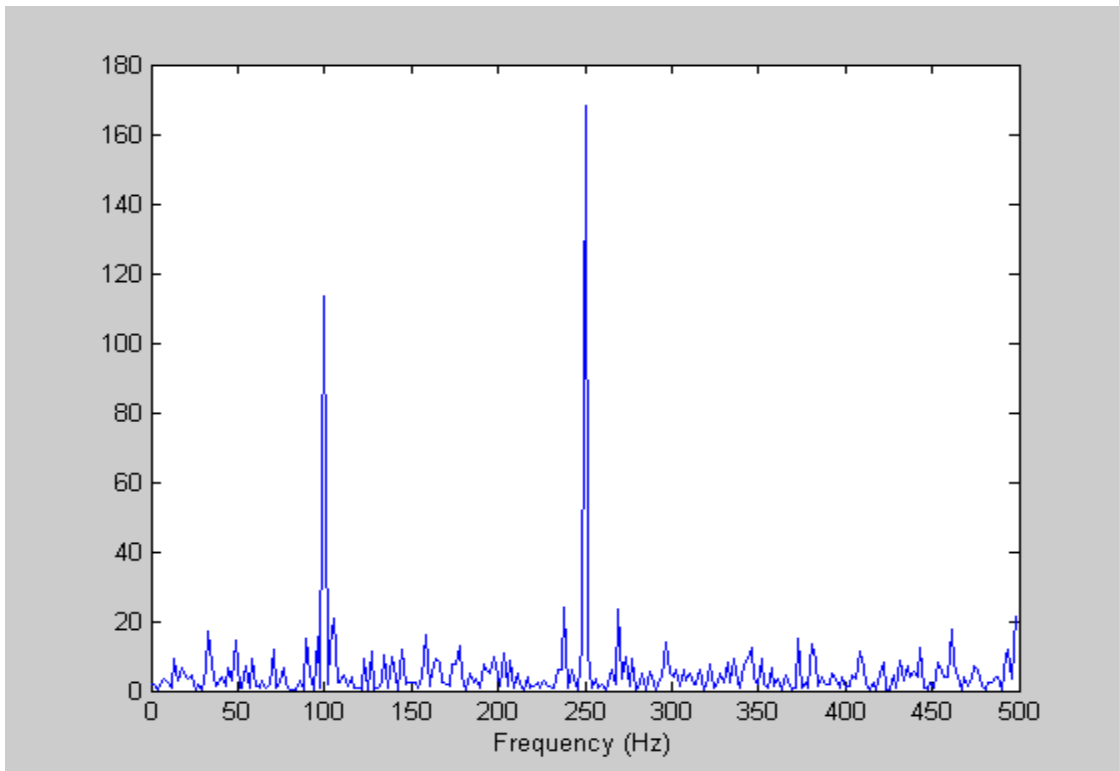


Figure 12: Fourier transform of nonuniform signal with frequency 100 and 250 Hz

4.2 Short term Fourier transform

In short-term Fourier transform (STFT), the signal is divided into small segments using a window function. For practical purposes the signal within each such segment can be assumed to be uniform. In this section an example is taken as a reference to explain (using (4.2), presented very shortly in this section), how STFT is calculated. To calculate

the STFT of a signal, the window function is placed at the beginning of the signal, for the period 't1' and the two are multiplied and the signal's (i.e. signal within the window) Fourier transform is found and this gives the frequency content of the signal for the time period 't1', next, the window is moved right to cover the segment of the signal for the time period 't2' and its Fourier transform is found. This procedure is repeated till the end of the signal is reached. This procedure gives the frequency content of the signal as well as the time information [11]. Figure 13 shows this above explanation pictorially.

STFT is used in this report to prove that the concept of ASM is applicable for load status monitoring inside a container/ trailer.

$$STFT(t', f) = \int_t [x(t) \cdot \omega^*(t-t')] e^{-j2\pi f t} dt \quad (4.2)$$

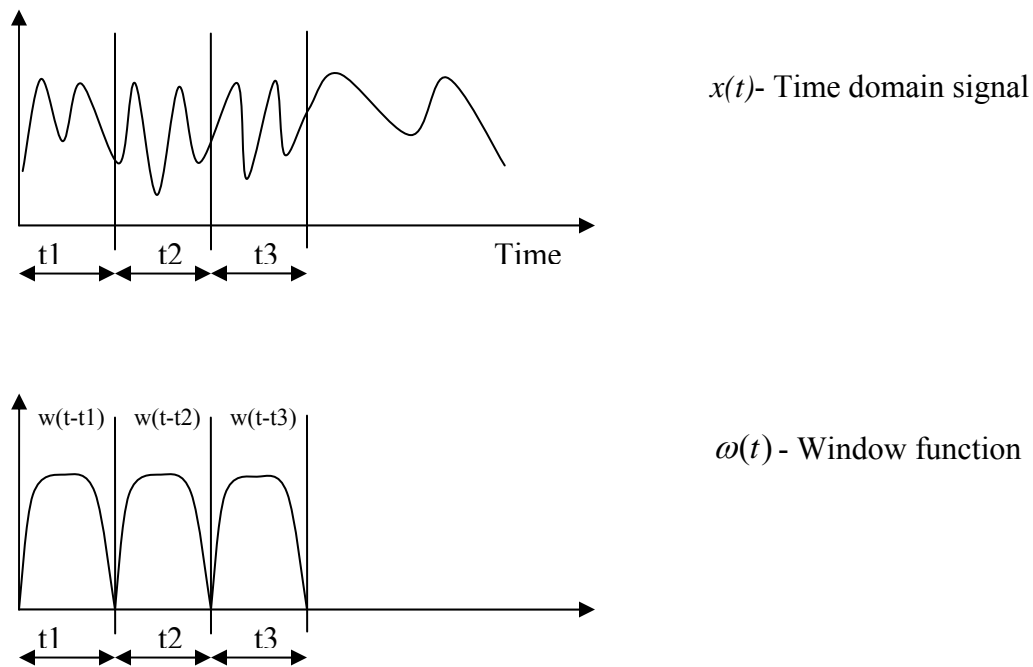


Figure 13: Example showing the calculation of STFT.

In practice sliding window technique is used to calculate STFT and is slightly different from what was explained earlier in this section. In the sliding window technique, the principle is to first decide on a window function and slide the window continuously and also overlap with the previous window. The percentage of overlap, the choice of window and window length and other parameters like FFT length depend on the application and its aim, i.e., to get a good time resolution or to get a good frequency resolution.

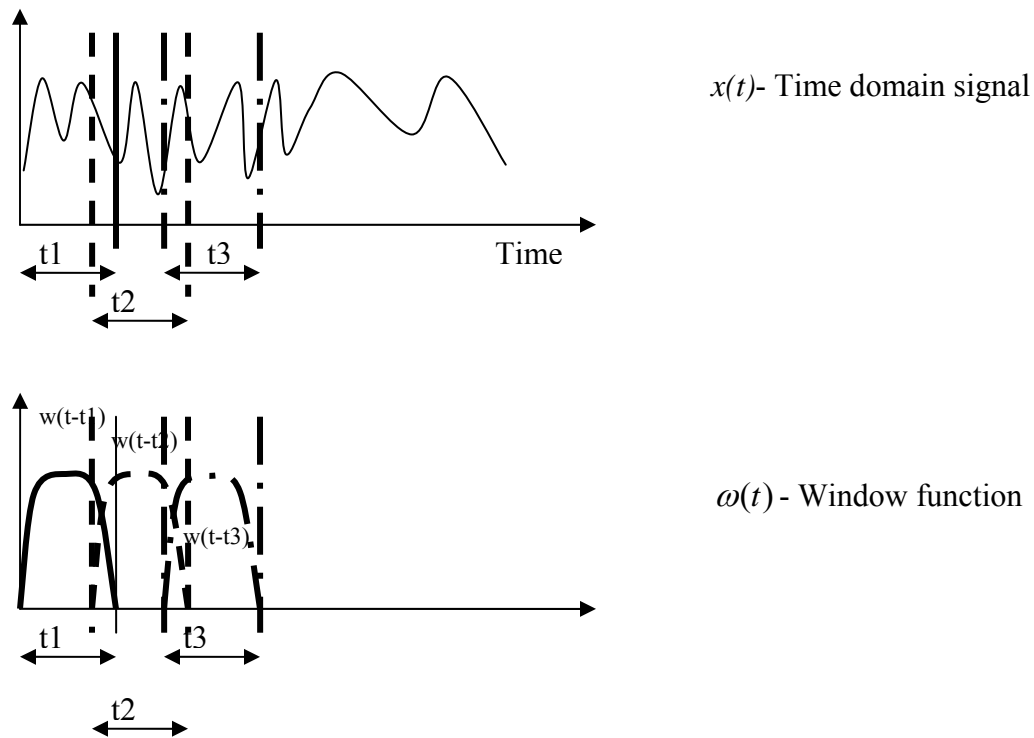


Figure 14: Calculation of STFT using sliding window method.

Comparing the two figures, Figure 13 and 14, we can see that there is overlapping of windows. In Figure 14 we can notice that, the second window for the period t_2 overlaps nearly 25% of the window for the period t_1 . The third window for the period t_3 overlaps nearly 25% of the second window for the period t_2 . MATLAB, a scientific mathematical

software tool for engineers, is used in this report to find the STFT of the collected signal samples. MATLAB's function "*spectrogram*" calculates STFT once it the input parameters like the signal, FFT length, value to produce 50% overlap and sampling frequency. The spectrogram function uses Hamming window. More information about this function can be found from MATLAB software help section. The actual values (in this report) used for the parameters in the spectrogram function are given in section 6.1 of chapter 6.

4.3 Wavelet transform:

Wavelet transform is a mathematical technique to find out time varying frequency information, similar to STFT. Detailed explanation of wavelet transforms is beyond the scope of this chapter and more information about wavelet transforms can be found in the appendix section.

5. FINDINGS: DATA AND DATA COLLECTION

5.1 Data collection:

This chapter shows the data samples collected and the method followed to obtain the data. The data obtained for analysis are echo samples. The echo samples were obtained from inside a trailer for different (four) load statuses with open/closed door conditions for each load status. The approximate dimensions of the trailer in which the data was collected are, length = 53 feet, width = 8 feet 10 inches and height = 8 feet. The load inside the trailer was banana pallets. Figure 15 shows the dimensions of the trailer/truck as well as the positions of the mic and acoustical excitation source (AES).

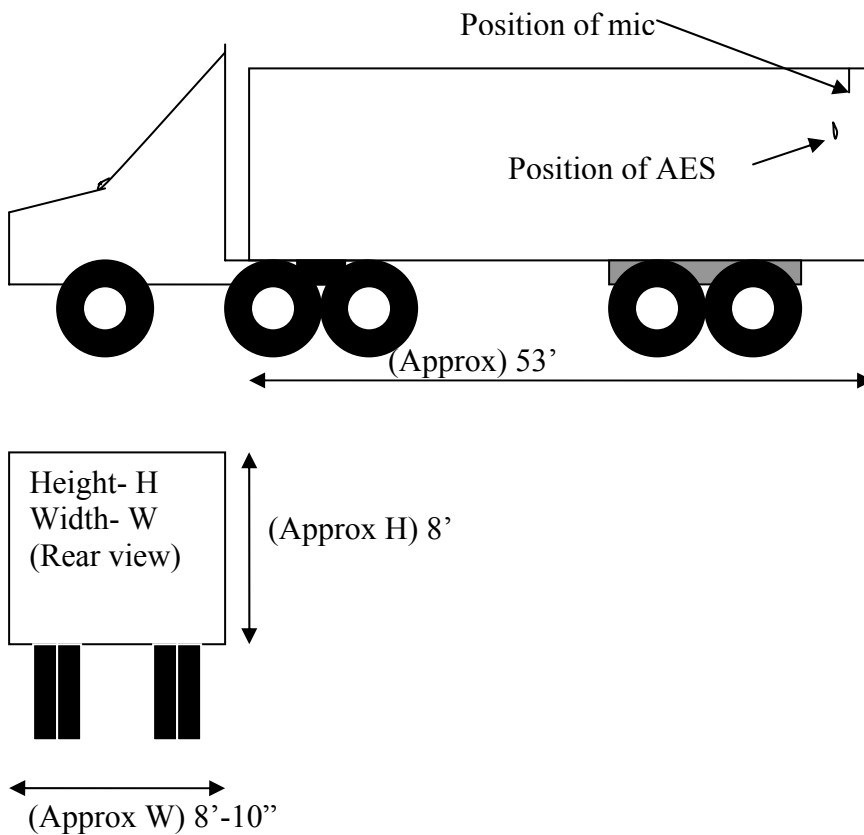


Figure 15: Figure showing the dimensions of the trailer/truck (side view and rear view) and positions of the mic and the acoustical excitation source (AES).

Two important factors that influence the echo are, load status and door open or closed condition. The different load status considered were, truck/trailer empty, one-third full (one third volume from front), two-thirds full (two-thirds volume from front) and full. For each of these cases the door condition was either open or closed. In other words there are a total of eight conditions and they are truck/trailer empty with doors closed, truck/trailer empty doors open, trailer one-third full doors closed, trailer one-third full doors open, trailer two-third full doors closed, trailer two-third full doors open, trailer full doors closed, trailer full doors open.

The samples collected through the receiver (mic) were stored on a laptop hard drive. For each of the previously mentioned eight different conditions, four samples were collected i.e. totally thirty-two samples were collected and analyzed. One sample for each condition is shown in the figures from Figure 16 to Figure 23. (Note: The signal length is not uniform for all the cases and hence the time scale is also not uniform.)

5.2 Actual data

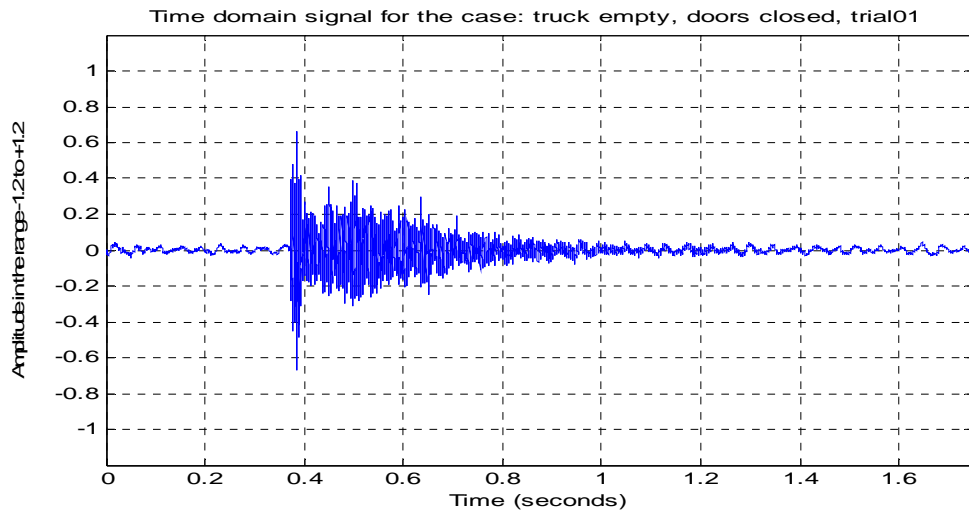


Figure 16: Echo sample for the case with truck/trailer empty, doors closed.

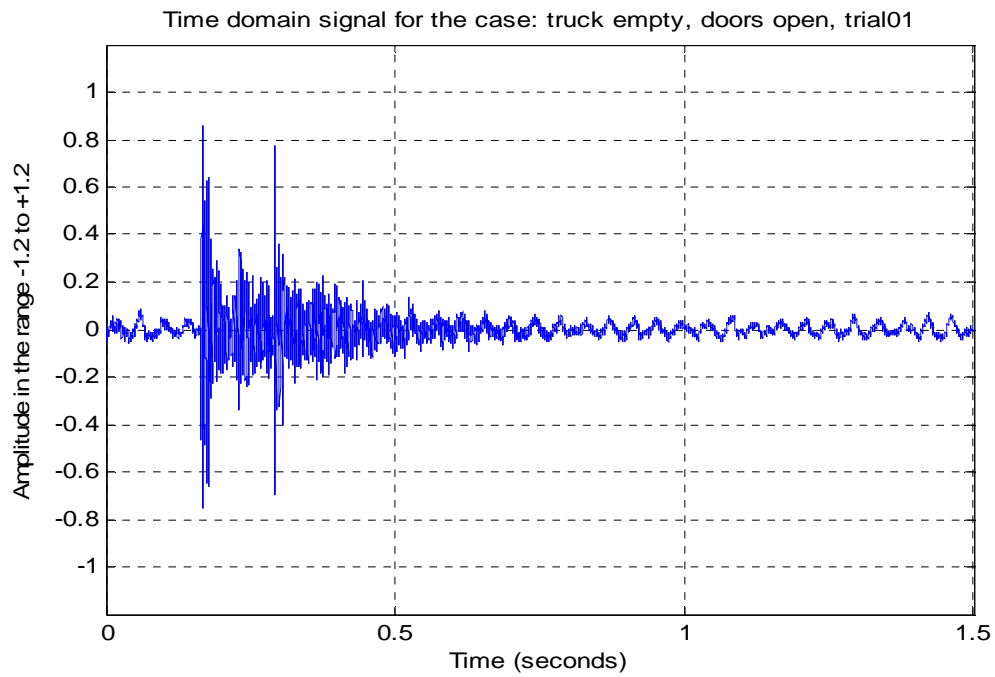


Figure 17: Echo sample for the case with truck/trailer empty doors open.



Figure 18: Echo sample for the case with trailer full doors closed.

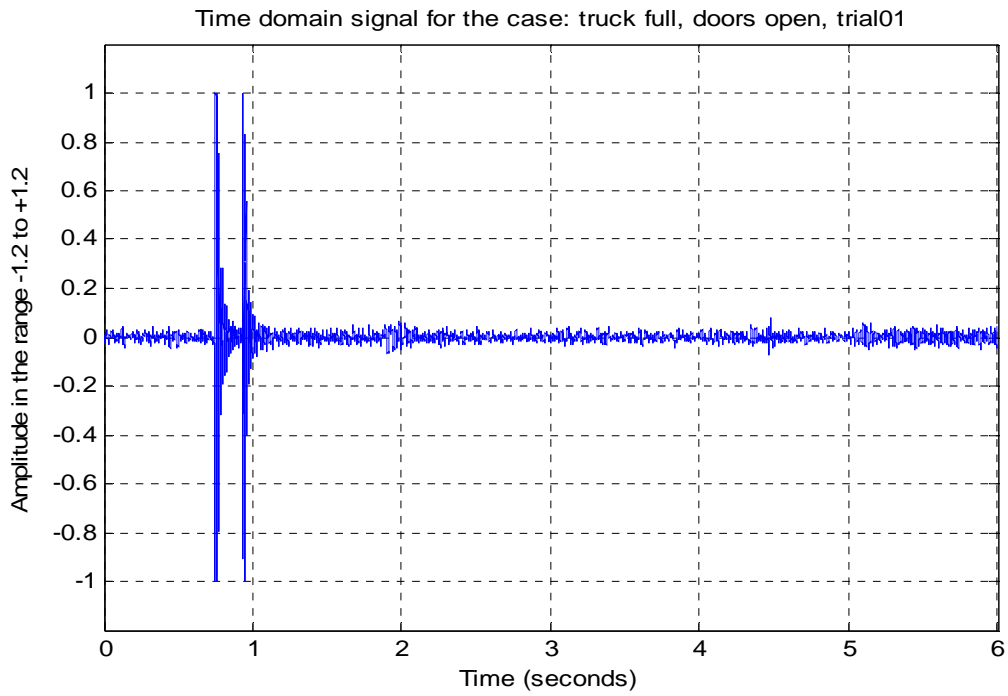


Figure 19: Echo sample for the case with trailer full doors open.

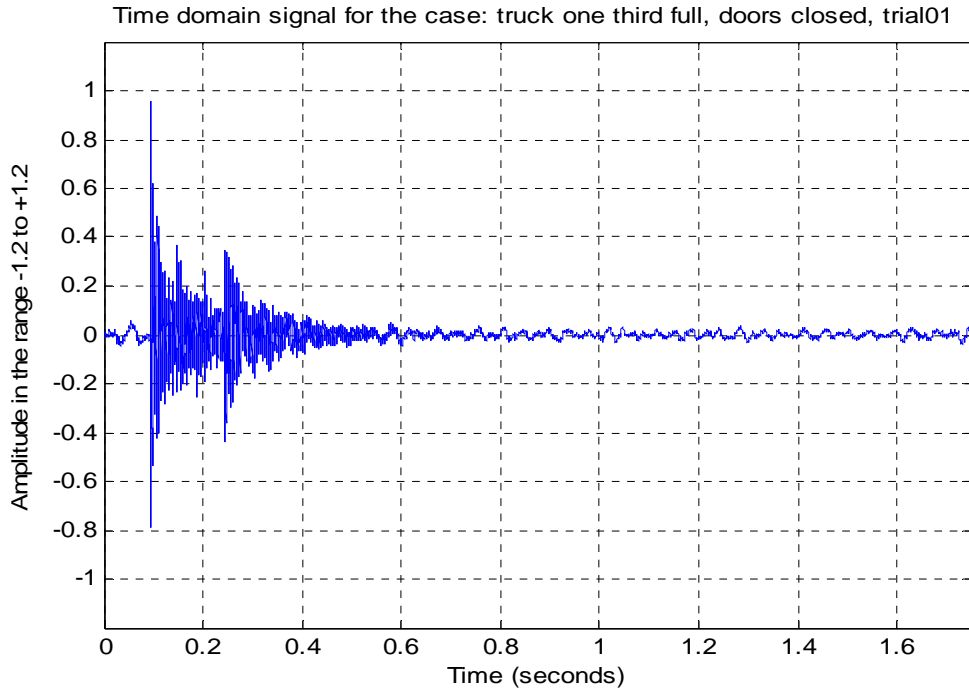


Figure 20: Echo sample for the case with trailer one-third full doors closed.

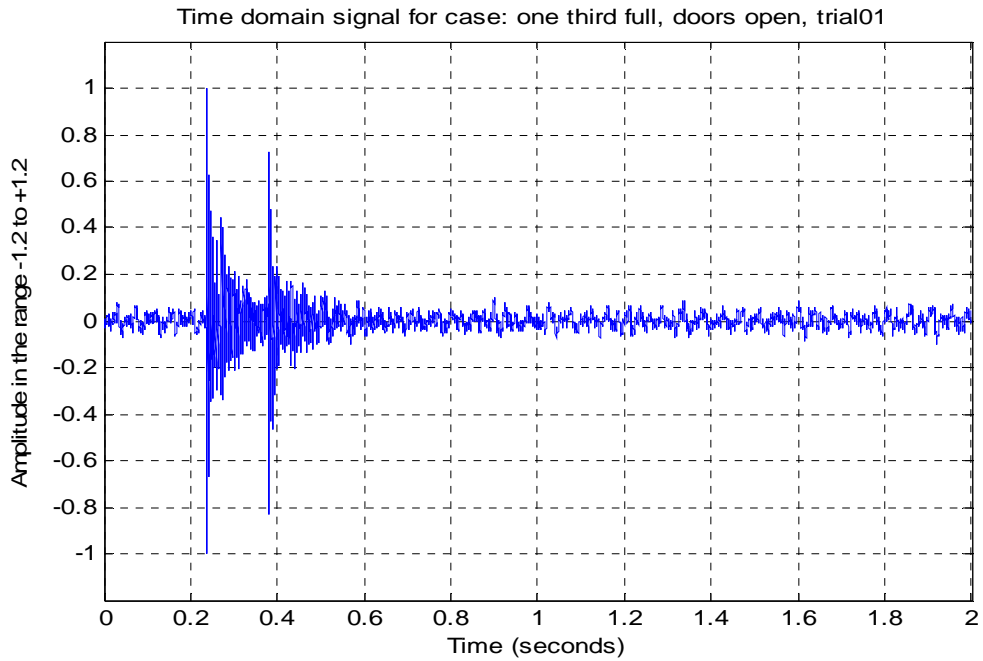


Figure 21: Echo sample for the case with trailer one-third full doors open.

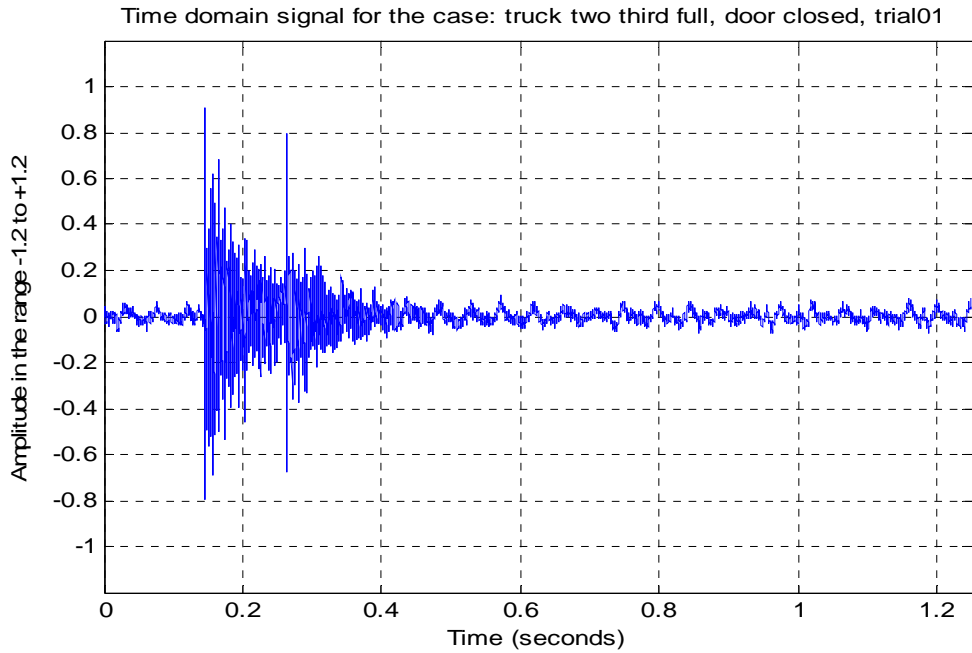


Figure 22: Echo sample for the case with trailer two-thirds full doors closed.

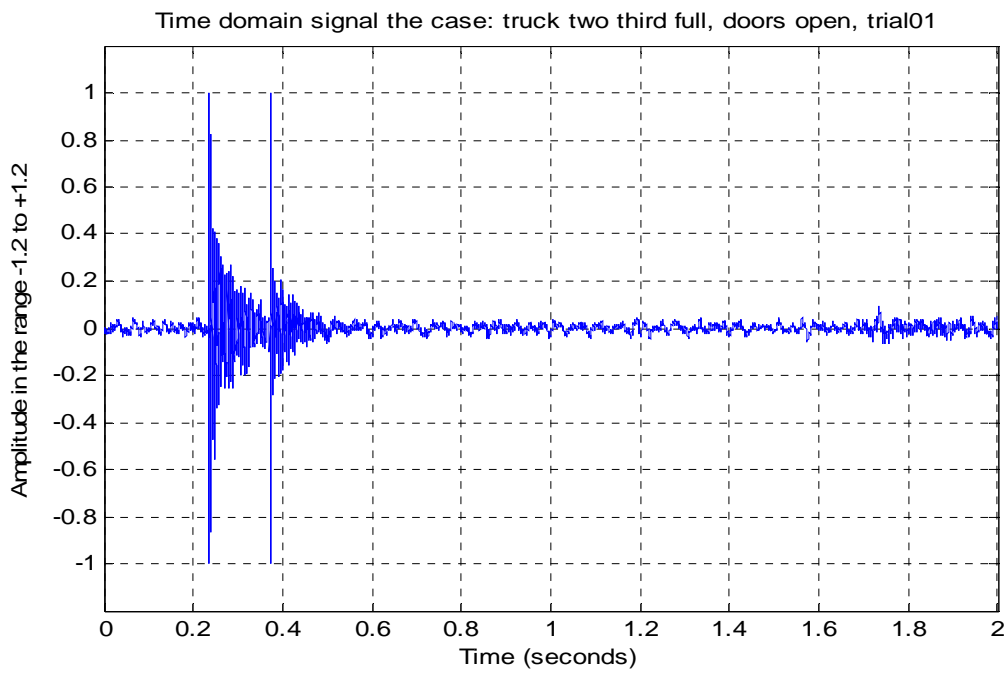


Figure 23: Echo sample for the case with trailer two-thirds full doors open

The 2 dimensional and 3 dimensional STFT figures of the above signals and detailed analysis of them are given in chapter 6.

6. ANALYSIS AND CONCLUSIONS

6.1 Graphical results

This chapter analyses the data obtained and also shows why Fourier transform (FFT) is not a suitable tool in analyzing nonuniform signals i.e. signals which has different frequencies at different times. The data samples have been shown in chapter 5, however Figures 16 and 17 have been reproduced here as Figures 24 and 25 for convenience.

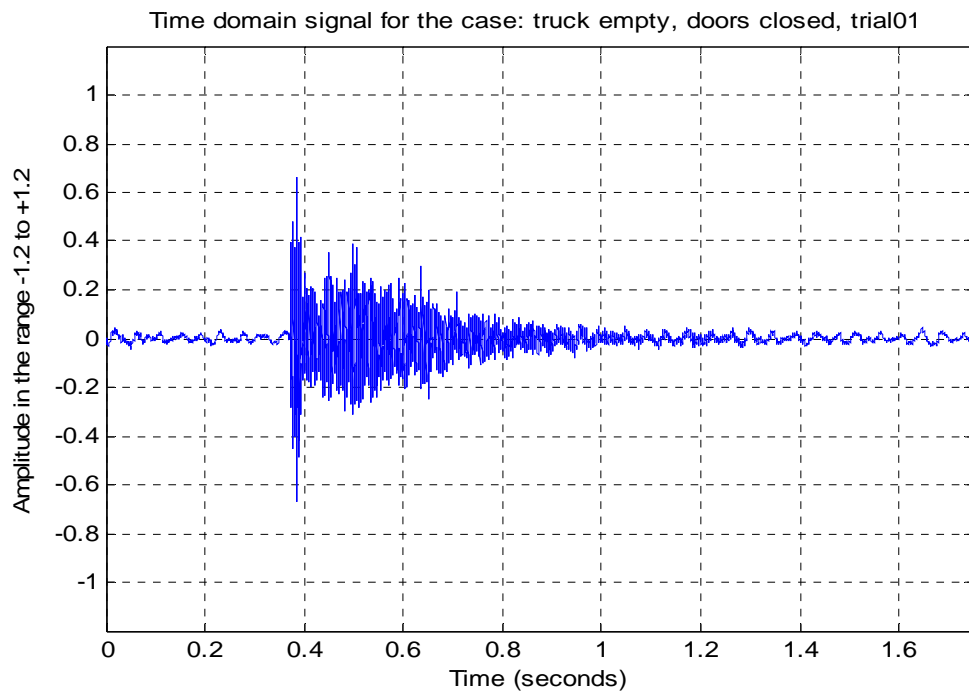


Figure 24: Echo sample for the case with truck empty door closed.

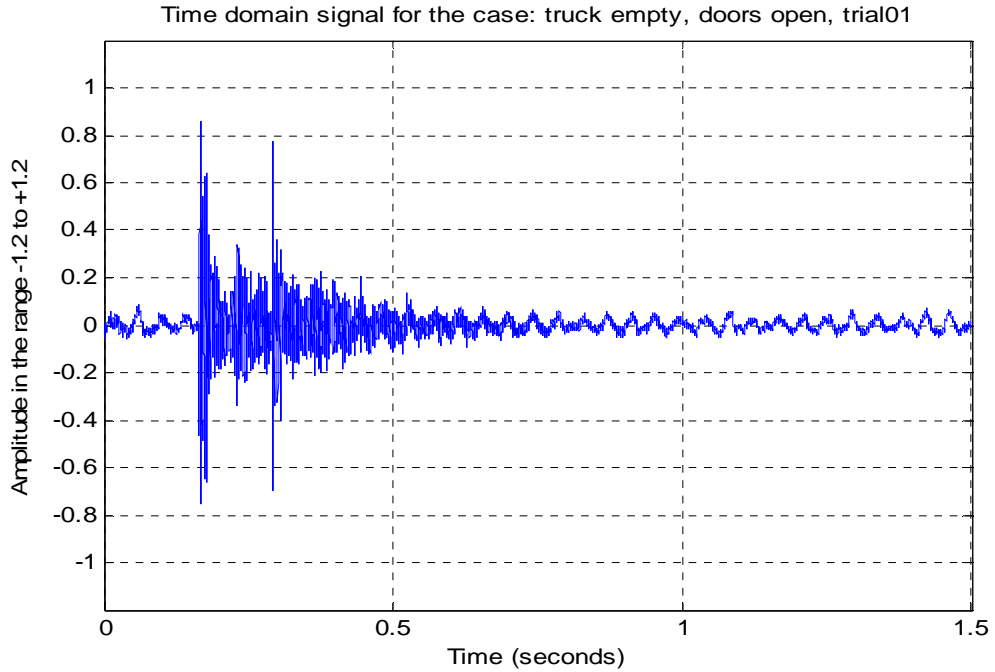


Figure 25: Echo sample for the case with trailer empty door open.

Fourier transforms of the two signals in Figures 24 and 25 are calculated using the method of FFT. The results are shown in Figure 26 and Figure 27 respectively on page 49. Figure 26 shows the FFT results logarithmic scale for both closed and open door condition and Figure 27 shows the FFT results in linear scale for both closed and open door condition.

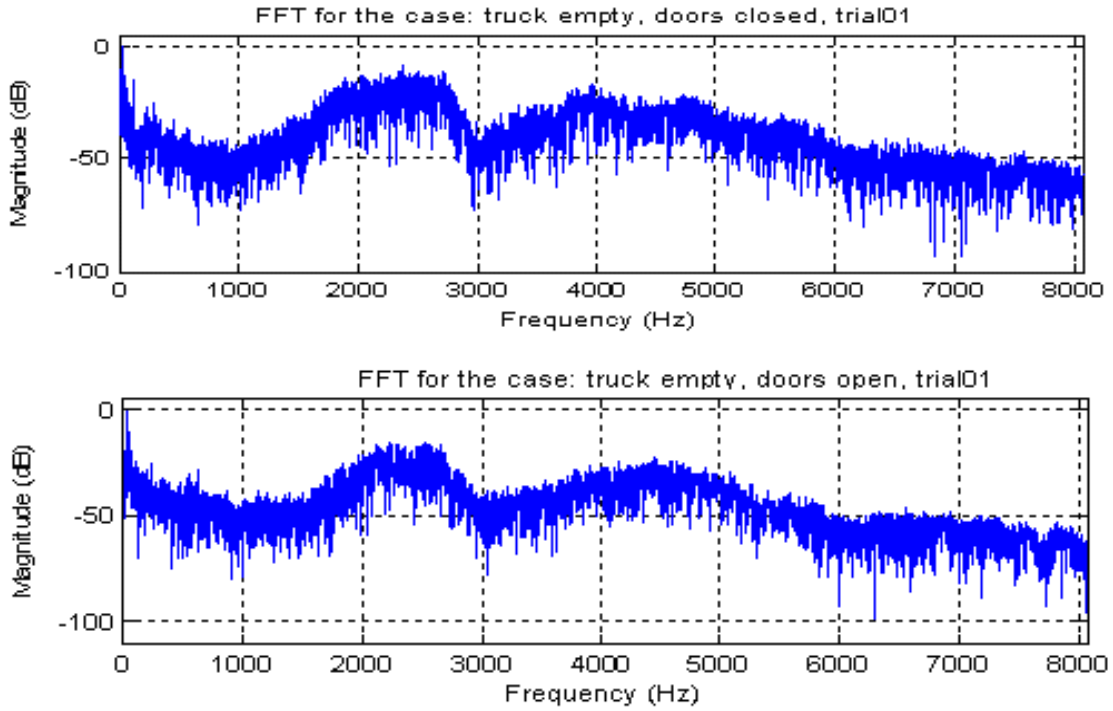


Figure 26: FFT, in logarithmic scale, of the time signals in Figure 24 and 25.

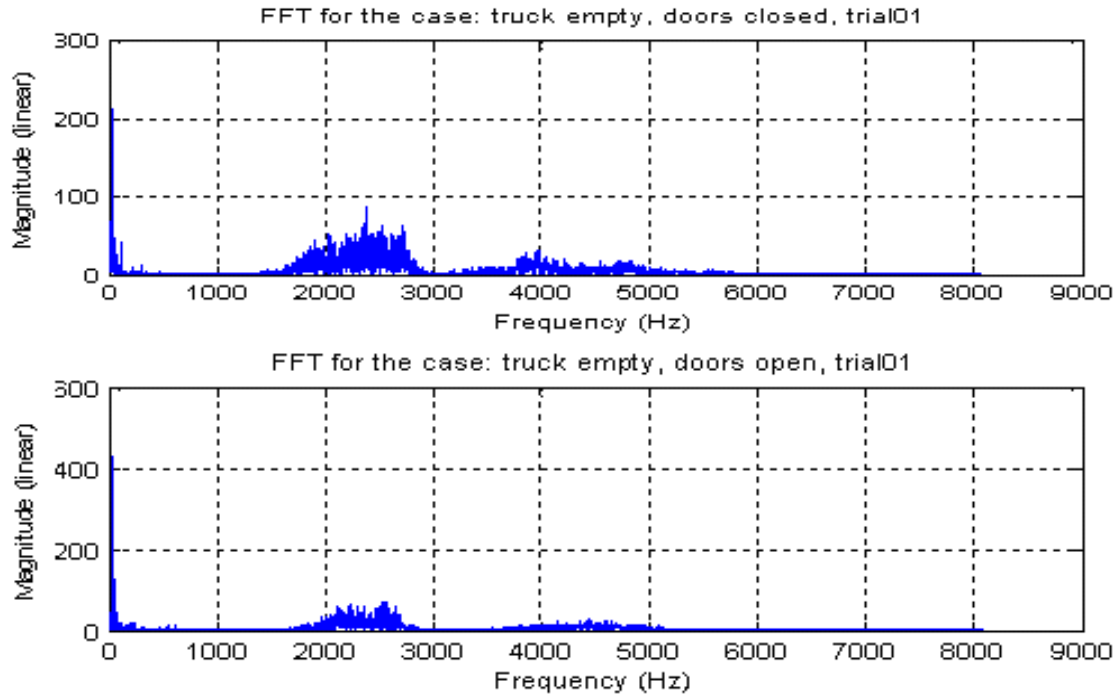


Figure 27: FFT, in linear scale, of the time signals in Figure 24 and 25.

The FFT length for the first signal in Figure 24 = 32768

The FFT length for the second signal in Figure 25 = 32768

The FFT shows the different frequencies present in each signal and the amplitude of each frequency component. From the two Figures 26 and 27, we can see that the correct analysis of the presence of the different frequency components is not possible with just the frequency information, because all the frequency components present in the first signal (Figure 24) also appear to be present in the second signal (Figure 25) and also there is no recognizable amplitude difference or any other pattern that can distinguish them.

Let us now consider short-term Fourier transform (STFT) of the same two signals in Figures 24 and 25, both two dimensional and three-dimensional plots are shown in Figures 28 to 31.

Spectrogram function from MATLAB has been used to plot the spectrogram (2 dimensional figure). The parameter values that were used are as given below:

- Window used: Hamming window (default) of length 256 (nfft)
- noverlap is the value that produces 50% overlap. noverlap = 250
- FFT length, nfft = 256
- Sampling frequency, $F_s = 22050$ Hz

Small value for FFT length, lower value for noverlap produced plots of spectrogram which were not very sharp. To get a sharper image different values for different parameters were tried and finally settled to the values given above which produced plots that were sharper enough to prove the distinctiveness.

The 2D and 3D plots are given here to show the effectiveness of STFT.

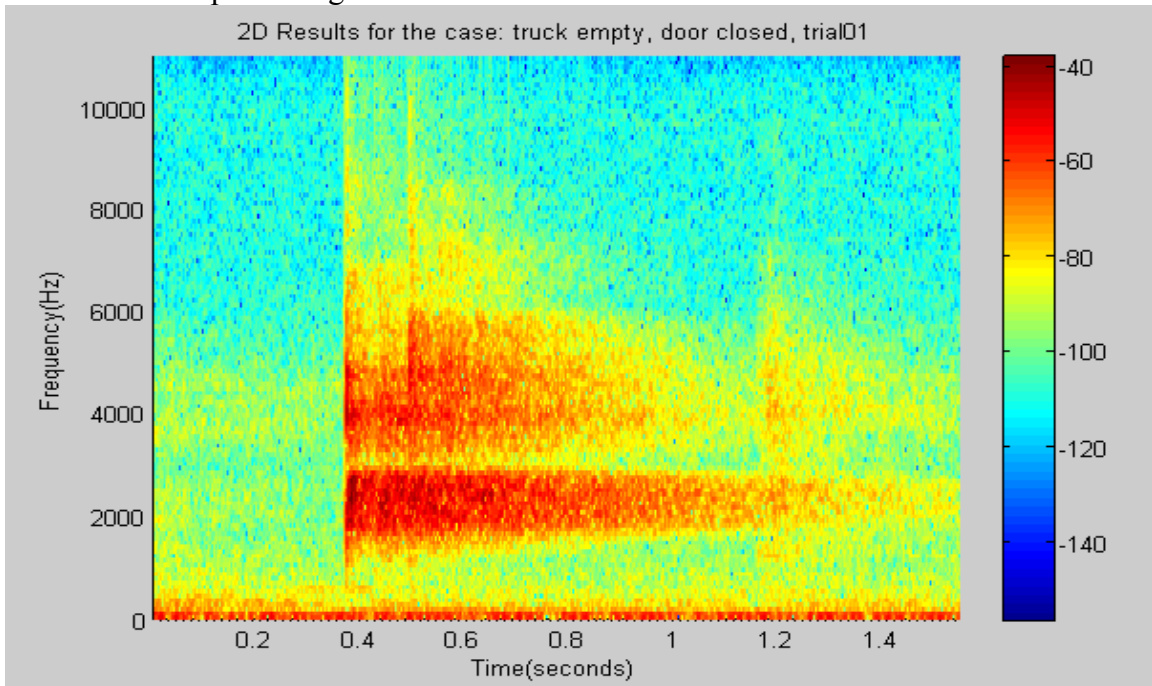


Figure 28: Two-dimensional plot of STFT for the signal in Figure 24 (truck/trailer empty doors closed).

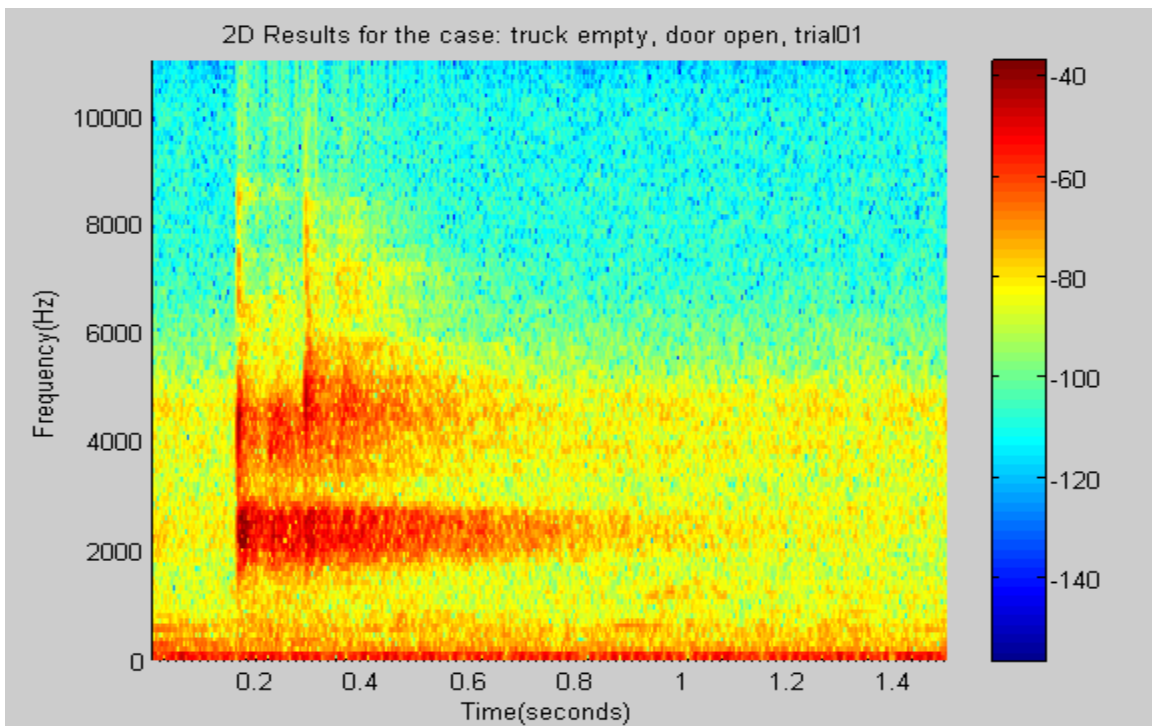


Figure 29: Two-dimensional plot of STFT for the signal in Figure 25 (truck/trailer empty doors open).

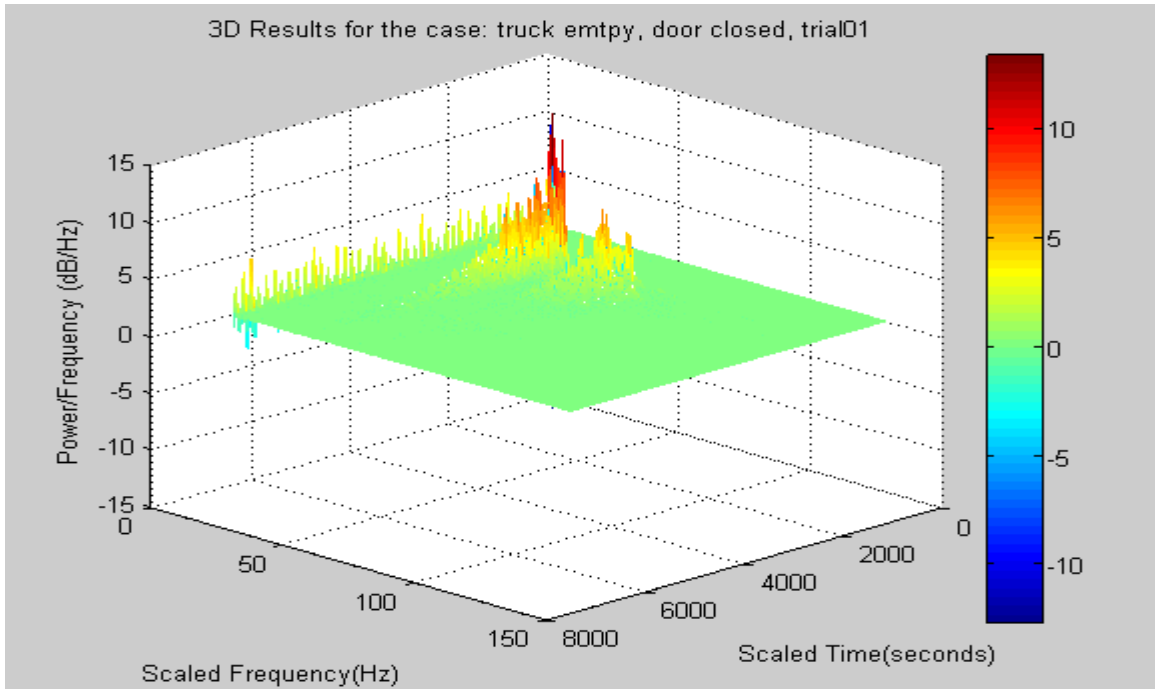


Figure 30: Three-dimensional plot of STFT for the signal in Figure 24 (truck/trailer empty doors closed)

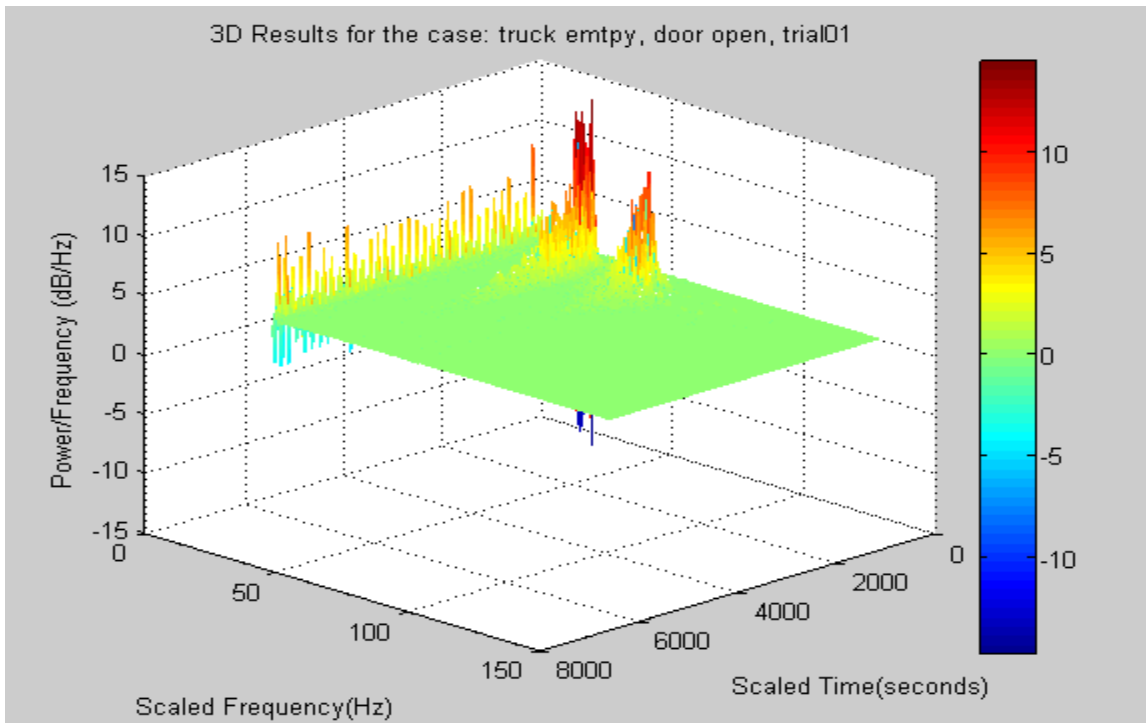


Figure 31: Three-dimensional plot of STFT for the signal in Figure 25 (truck/trailer empty doors open)

The time and frequency axes in the three dimensional figures given in Figure 30 and 31 are scaled. The scaled frequency and time axes' details are given below:

Scaled frequency axis details for the Figure 30: 1 division = 73.5 Hz

Scaled time axis details for the Figure 30: 1 division = 0.218 msec

Scaled frequency axis details for the Figure 31: 1 division = 73.5 Hz

Scaled time axis details for the Figure 31: 1 division = 0.249 msec

Close observation of the Figures 28 to 31 shows that, the rate of decay of different frequencies in case of the first signal is slower compared to the rate of decay of different frequencies in case of the second signal. The reason for this difference in the rates of decay is because, in case of the first signal the door was closed and the truck was empty, leading to a condition where the sound could travel the entire length of the trailer multiple number of times. In the second case since the door was open, much of the sound could escape through the open doors before the sound could travel multiple numbers of times through the entire length of the trailer. In other words in case of the first signal there were multiple reflections or prolonged reverberations leading to slow decay of different frequency components, however in the second case, there were not considerable number of reflections and the echoes died quickly leading to a faster rate of decay of different frequency components.

Section 6.2 on page 55 shows two dimensional and three dimensional plots (Figures 32 to 43) for the remaining six conditions, truck one-third full door closed, truck one-third full door open, truck two-thirds full door closed, truck two-thirds full door open, truck full door closed, truck full door open. Section 6.2.1 explains about the information associated with 2D and 3D graphs in detail.

6.2 Two and Three dimensional plots for the remaining conditions:

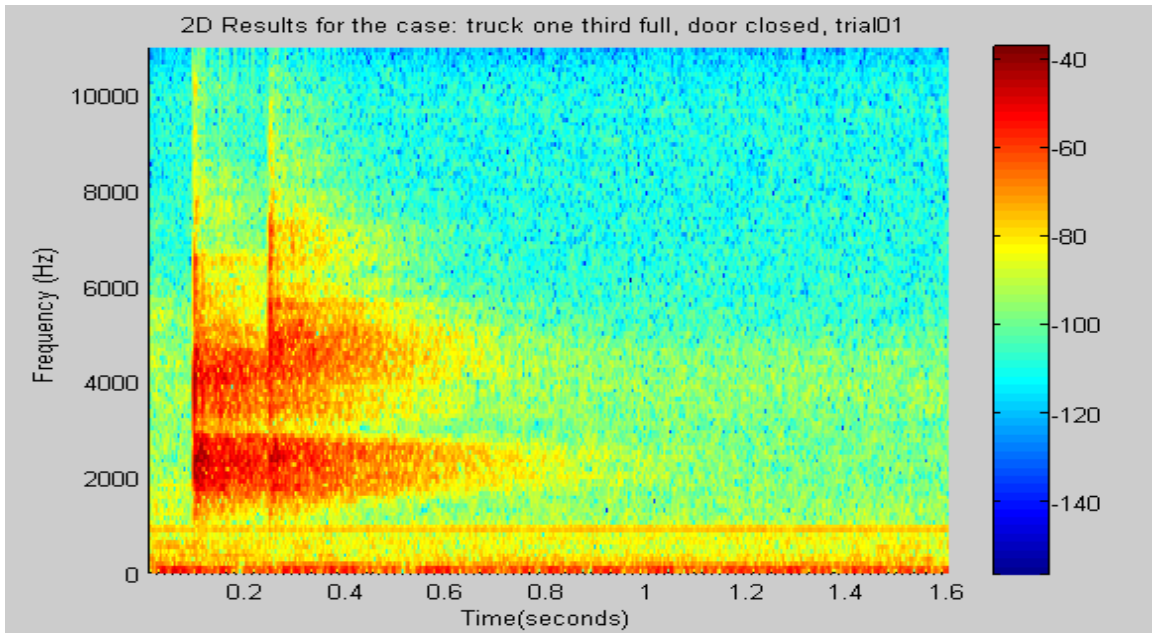


Figure 32: Two dimensional plot for the case with truck one-third full doors closed.

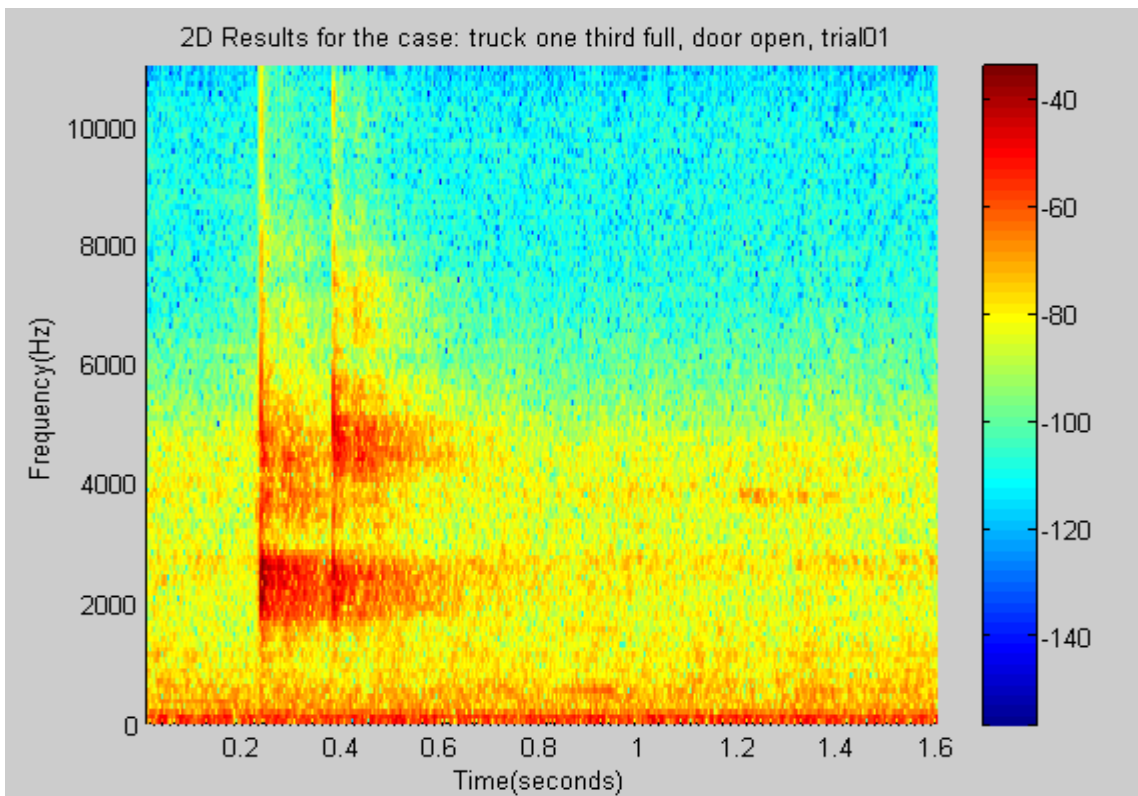


Figure 33: Two dimensional plot for the case with truck one-third full doors open.

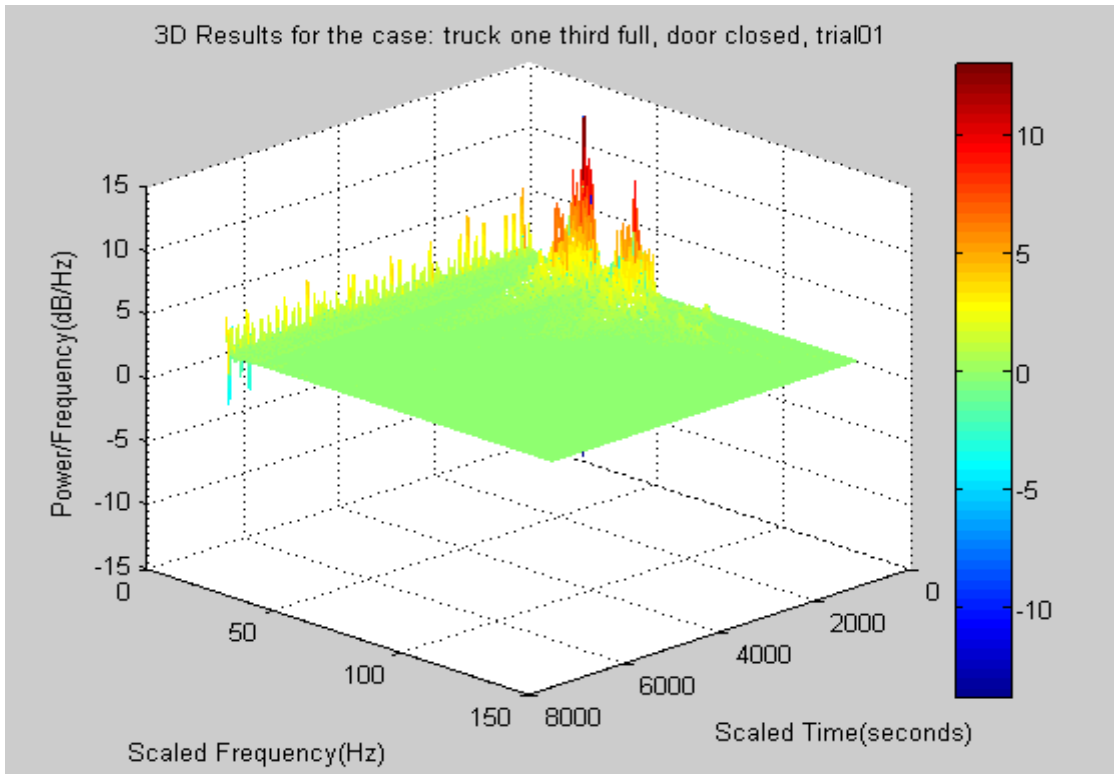


Figure 34: Three dimensional plot for the case with truck one-third full doors closed.

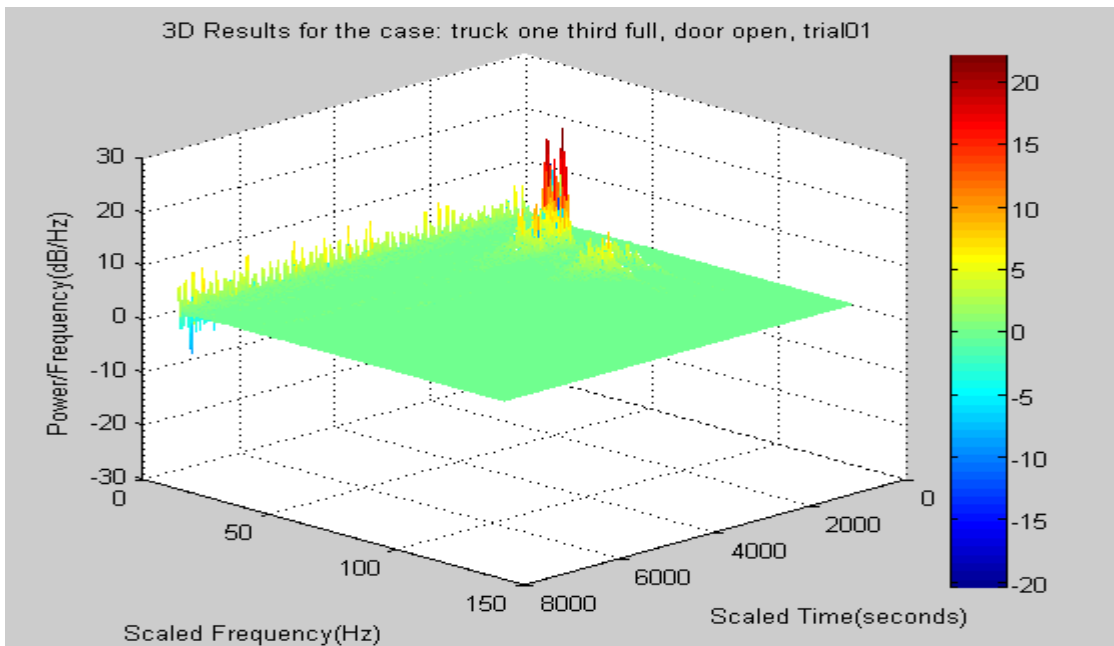


Figure 35: Three dimensional plot for the case with truck one-third full doors open.

Scaled frequency axis details for the Figure 34: 1 division = 73.5 Hz

Scaled time axis details for the Figure 34: 1 division = 0.218 msec

Scaled frequency axis details for the Figure 35: 1 division = 73.5 Hz

Scaled time axis details for the Figure 35: 1 division = 0.249 msec

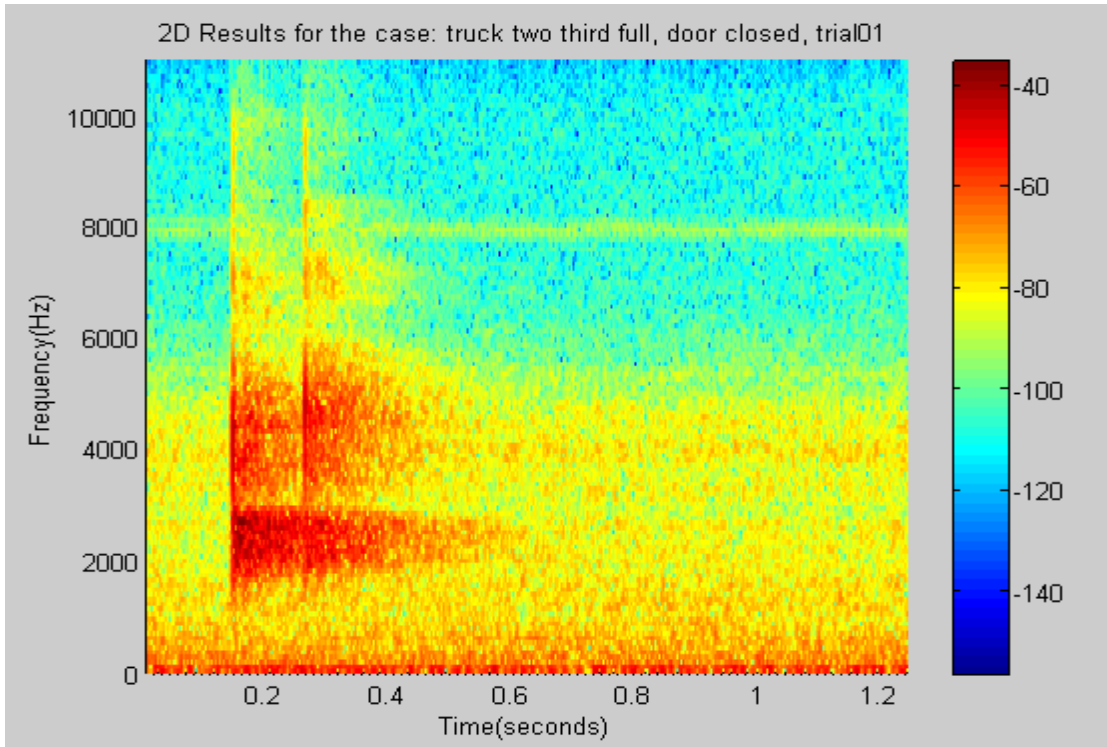


Figure 36: Two dimensional plot for the case with truck two-thirds full doors closed.

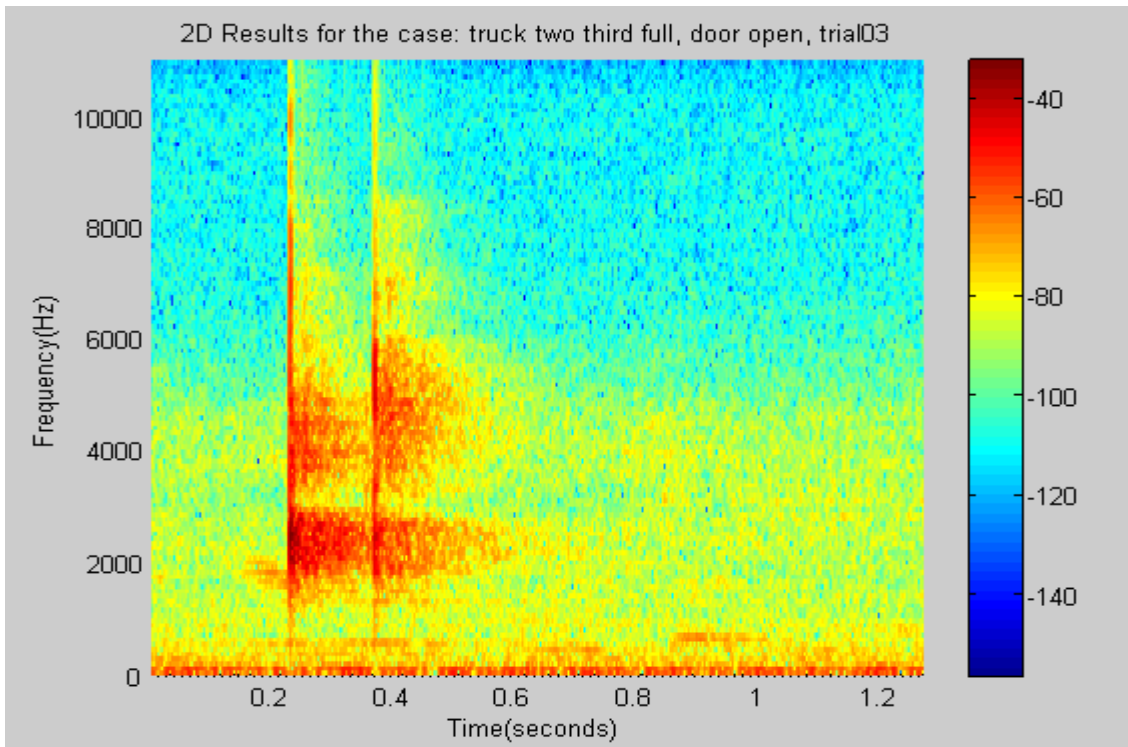


Figure 37: Two dimensional plot for the case with truck two-thirds full doors open.

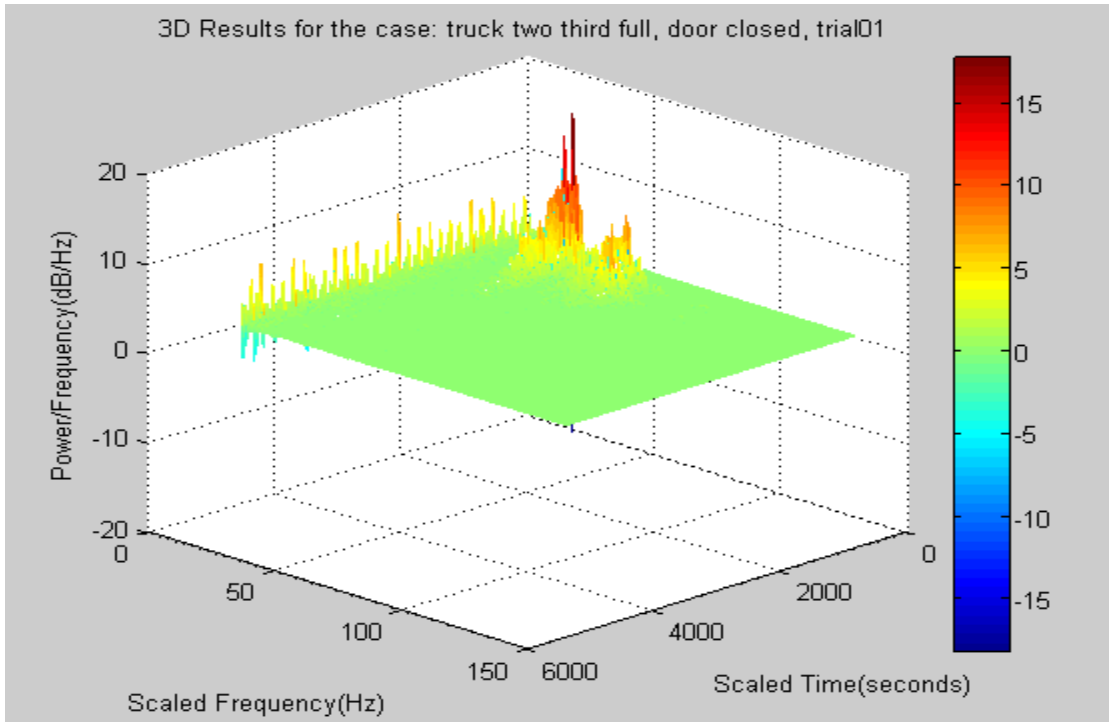


Figure 38: Three dimensional plot for the case with truck two-thirds full doors closed.

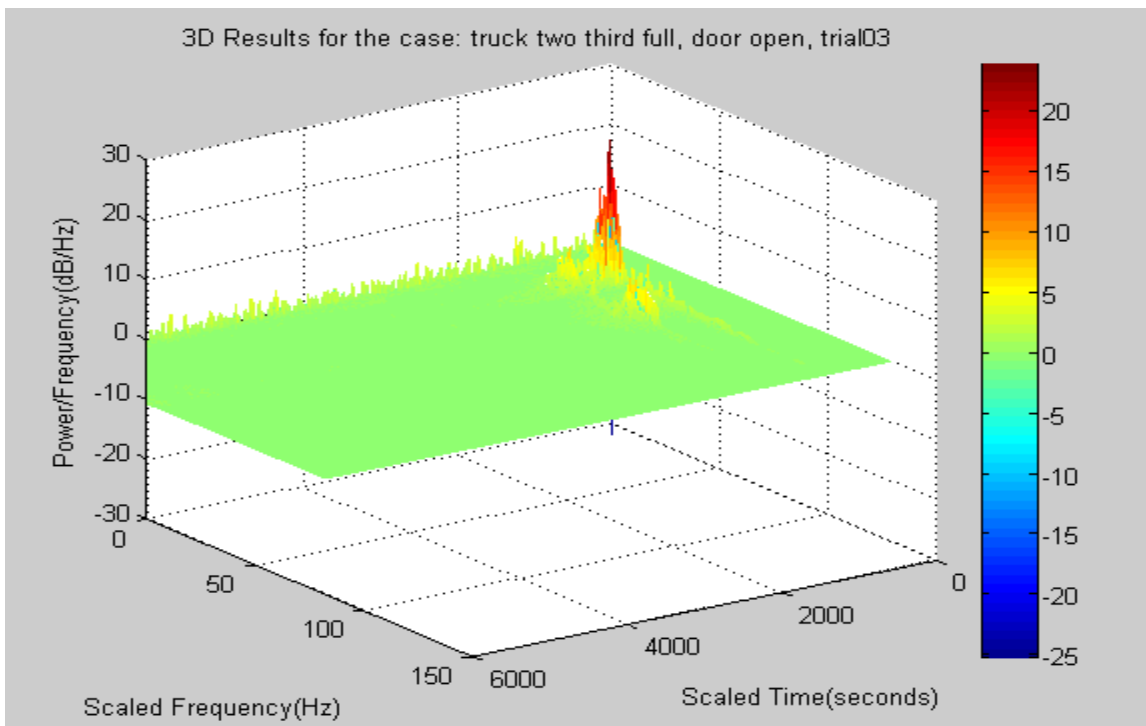


Figure 39: Three dimensional plot for the case with truck two-thirds full doors open.

Scaled frequency axis details for the Figure 38: 1 division = 73.5 Hz

Scaled time axis details for the Figure 39: 1 division = 0.207 msec

Scaled frequency axis details for the Figure 39: 1 division = 73.5 Hz

Scaled time axis details For the Figure 39: 1 division = 0.249 msec

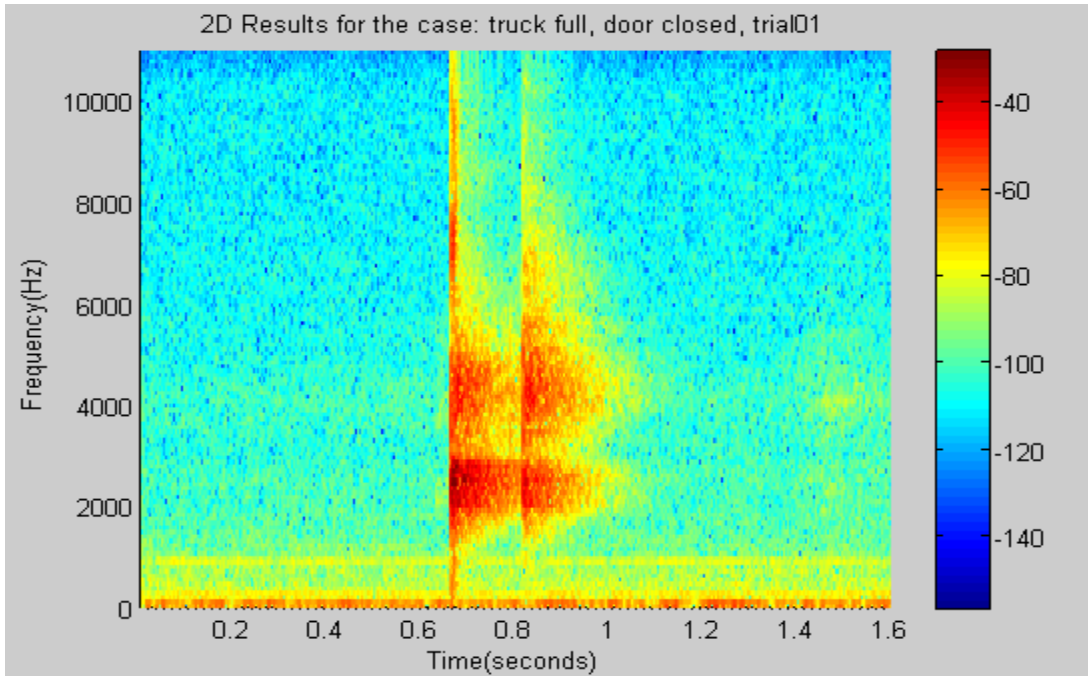


Figure 40: Two dimensional plot for the case with truck full doors closed.

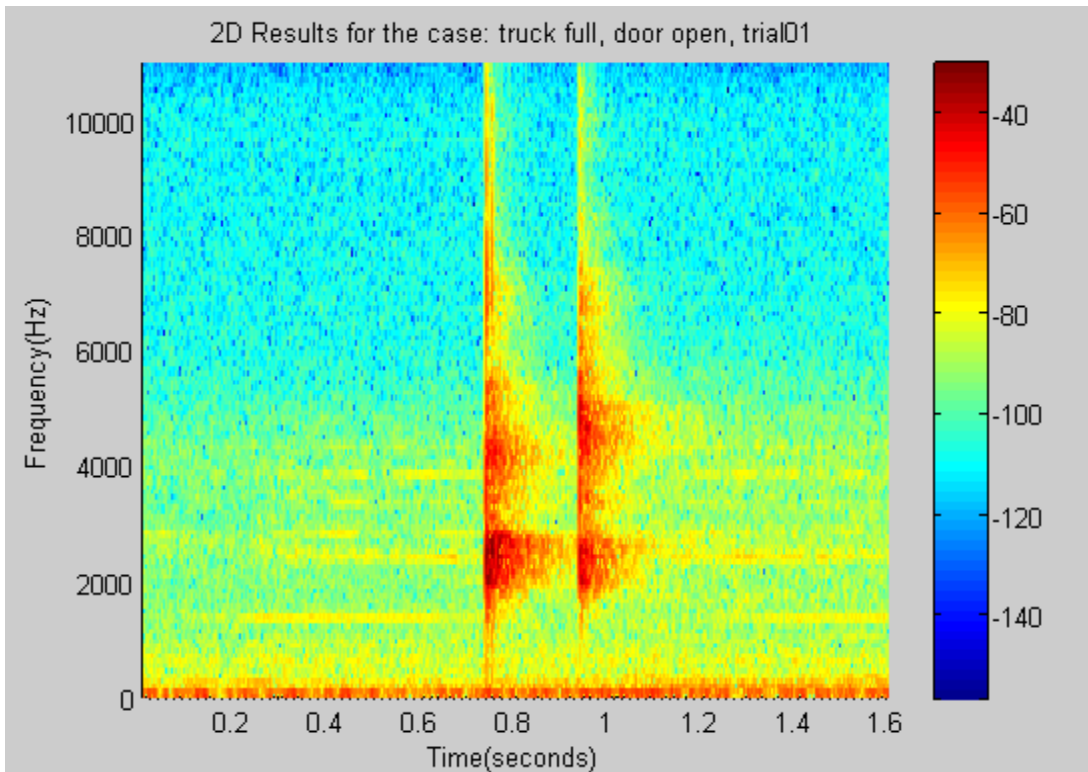


Figure 41: Two dimensional plot for the case with truck full doors open.

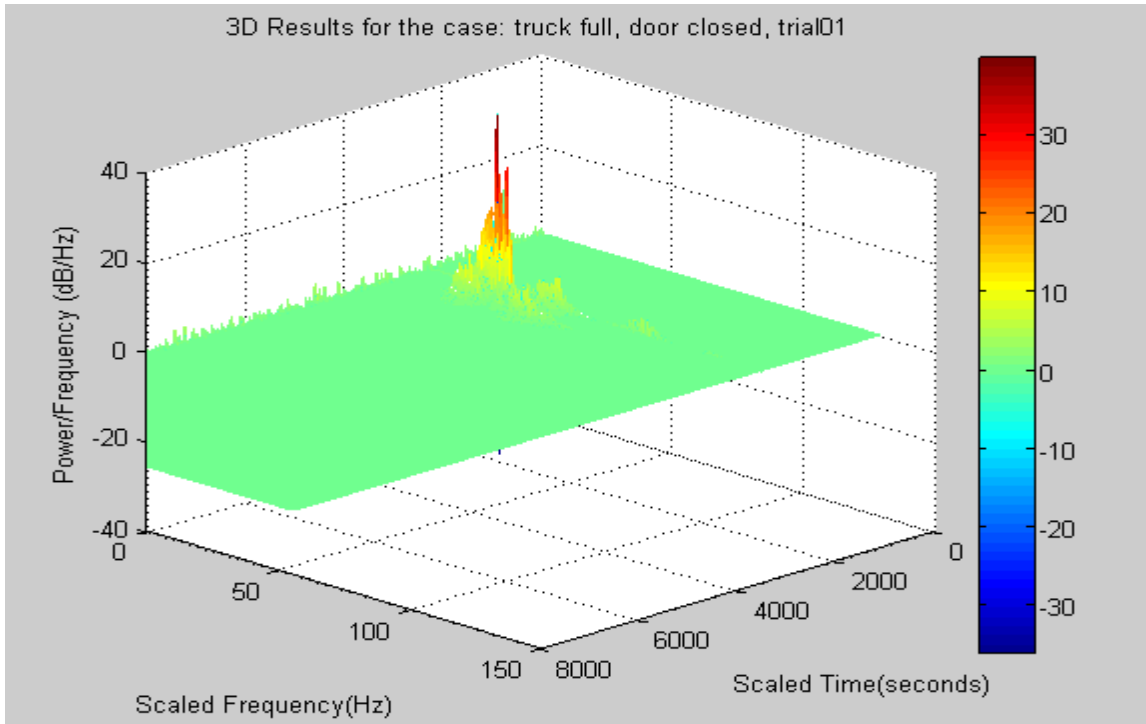


Figure 42: Three dimensional plot for the case with truck full doors closed.

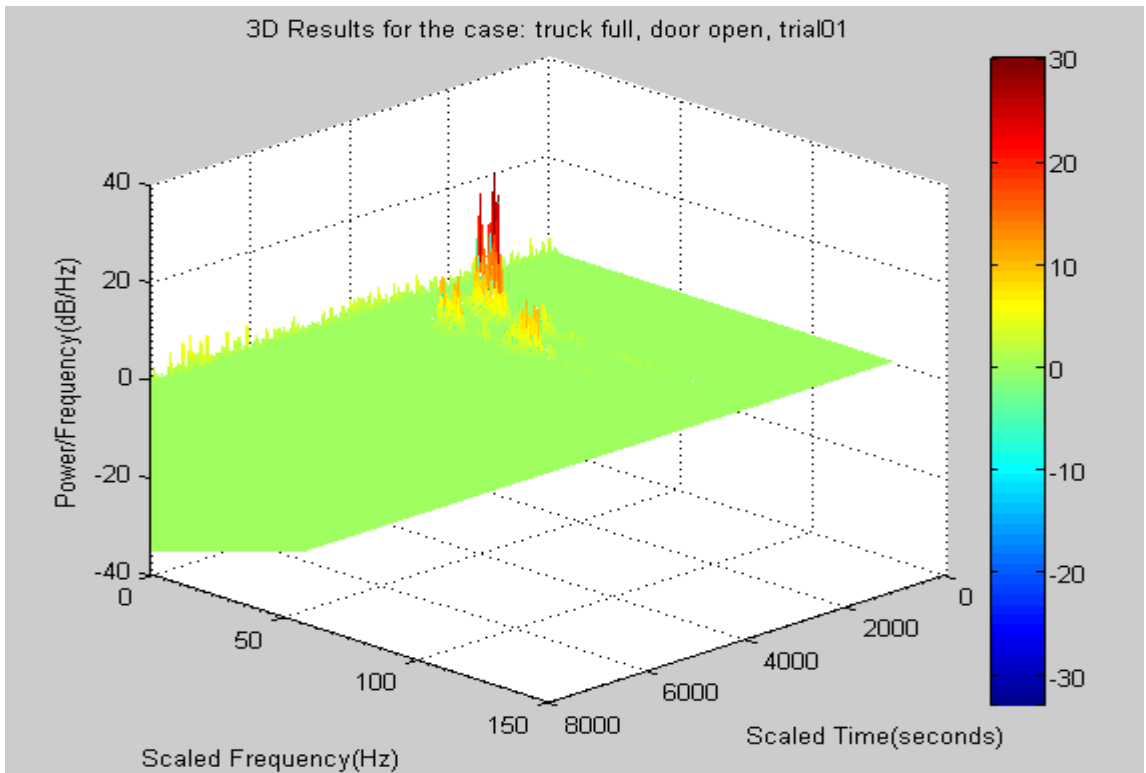


Figure 43: Three dimensional plot for the case with truck full doors open.

Scaled frequency axis details for the Figure 42: 1 division = 73.5 Hz

Scaled time axis details for the Figure 42: 1 division = 0.216 msec

Scaled frequency axis details for the Figure 43: 1 division = 73.5 Hz

Scaled time axis details for the Figure 43: 1 division = 0.239 msec

6.2.1 Analysis of 2D and 3D graphical results

This section explains what the 2D and 3D plots mean, how they are plotted and how these prove the concept of ASM.

The input is an analog signal which is stored in the hard drive of a laptop in digital format, and the digital format used in this case is 16 bit PCM (pulse code modulation) with a sampling frequency of 22050 Hz. After sampling the signal, only a sequence of numbers is stored on the hard drive of the computer. In the next stage the windowed frequency spectrum of the signal (collected sequence) is found in order to know the magnitude of different frequencies at different instants of time. This is done by finding the STFT of the signal. MATLAB software is used to find the windowed spectrum of the signals and also to plot 3D figures.

Spectrogram refers to the frequency spectrum of a signal, the difference (compared to regular spectrums) is that, in this case the frequency spectrum is found from the windowed frames of the signal. In other words, spectrogram can be said to be the result

of applying the technique of STFT on the signal. The way spectrogram function in MATLAB works is explained here. This function calculates the STFT of the signal and it also returns a matrix containing the power spectral density (PSD) of each segment of the signal, and the function then plots this PSD estimate. The dimensions of PSD is power per unit frequency or power per radians per sample. From the description of spectrogram given above we can say that, spectrogram plots represent the square of the magnitude of the STFT of each segment of the sequence under consideration. The way spectrogram function in MATLAB calculates the STFT needs a little more explanation here. As mentioned earlier *Spectrogram* function returns a matrix containing the power spectral density of the signal segments, however the input signal in this case is real (sequence of numbers), so the matrix returned by the *spectrogram* function contains one sided estimate of the PSD of each segment. To calculate the PSD, MATLAB uses its own algorithm described on the following lines (more information about this can be found in the MATLAB help section).

Let x be a sequence $[x_1, x_2, \dots, x_n]$

The periodogram (periodogram is a MATLAB function that returns PSD of the input sequence) for the above sequence is given by $\frac{S(e^{j\omega})}{F}$, where

$$S(e^{j\omega}) = \frac{1}{n} \left(\sum_{l=1}^n x_l e^{-j\omega l} \right)^2$$

n is the maximum length of the sequence x , l represents the index. F is the sampling frequency (if it is supplied) or 2π (if the sampling frequency is not supplied) [9]. Since the sampling frequency is supplied by the spectrogram function, $S(e^{j\omega})$ is divided by the sampling frequency, which is 22050 Hz in this case. The resulting value is expressed in

decibels, which is a logarithmic unit. This explains for the low negative values. An important point needs to be mentioned here about the value being expressed in decibels. This decibel value doesn't represent the actual power of the input signal. To know the actual power, we need to calculate sound power level (appendix B). While calculating spectrogram values, MATLAB calculates the value of periodogram divided by sampling frequency (which is basically just a number of very small magnitude) and then expresses that number in logarithmic units called decibels. More explanation is given in appendix B on how to calculate the actual power of a signal.

The color coding schemes in 2D and 3D plots show different amplitude levels for the same condition and there by they appear to convey that 2D and 3D plots are representing different signals. The change in the amplitude values in the 2D and 3D plots is due to the difference in the scaling of the values to the color map. The 2D plot is done by the function '*surf*' of MATLAB and the 3D plot is done by '*mesh*' of MATLAB and for each of these functions the color scaling scheme is different. The function '*caxis*' does the job of mapping the data values to the color-map. '*caxis*' sets the color limits to a specified minimum (Cmin) and maximum (Cmax) values. Data values less than or greater than these specified values are assigned to the specified minimum and maximum values itself. The minimum (Cmin) and maximum (Cmax) values are mapped to the first and last color value in the color-map. The last color on the color-map (RGB) is always blue and the first color is red. If we consider the Surf function, the range of the axes determines the color scaling. This color scaling is different for Mesh function. Since, Surf (for 2D plot) and Mesh (for 3D plot) have different color scaling and color mapping schemes, the color

coding scheme for 2D and 3D plot is different and hence the difference in amplitude values. Figures 44 and 45 show the color-map-editor for 2D and 3D for the case ‘truck empty and doors closed’. The parameters and the values to look at are the “index” and “CData” under the title ‘Current color info’ and “Color data min” and “Color data max”.

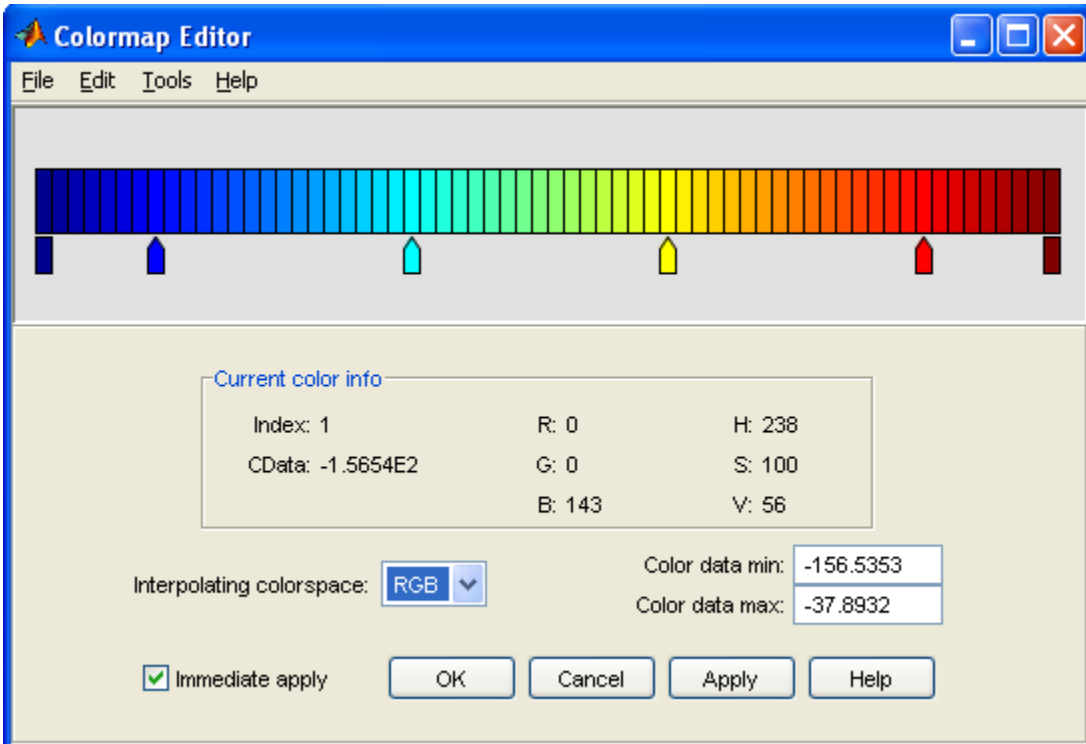


Figure 44: Color-map-editor for 2D plot for the case truck empty and door closed

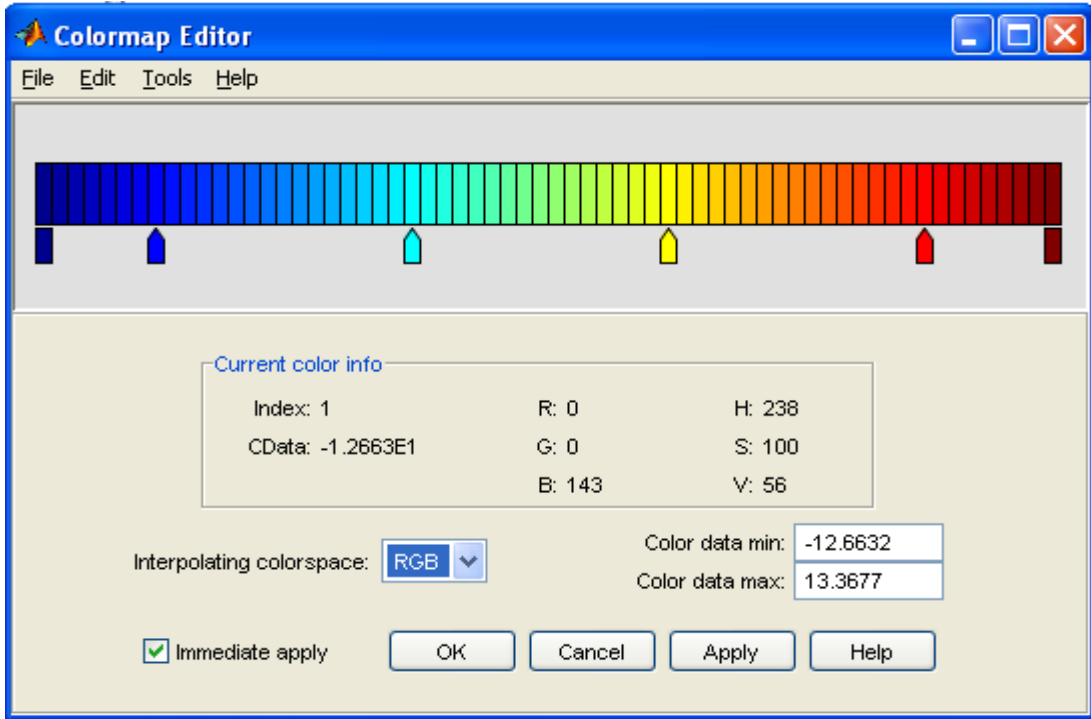


Figure 45: Color-map-editor for 3D plot for the case truck empty and door closed.

Though the above figures (Figures 44 and 45) are for the case, “truck empty doors closed”, the explanation of different color coding schemes for 2D and 3D plots hold true for the rest seven cases.

6.3 Conclusion

The resonant frequency of an air cavity is inversely proportional to the volume inside the cavity. If the volume is large then the resonant frequency is lower since more quantity of air has to move and if the volume is less then the resonant frequency is higher as less quantity of air has to move. The resonant frequency is also dependent directly on the area

of the opening of the cavity. If the area of the opening is large then the air can move in and out easily and hence the resonant frequency increases and if the area of the opening is small then the resonant frequency is lower as the movement of air is slower. This same principle can be applied to a trailer/container having different volumes of load and door open and closed condition. When the trailer is empty with the door closed, the volume of air cavity is large and hence the resonant frequency is lower. When the trailer is empty and the door is open the resonant frequency is higher. Similarly when the load is one thirds or two-thirds and the door is closed or open the resonant frequency changes accordingly. Apart from the changes in the resonant frequencies, each condition of the trailer/container will have different volume of air cavity and because of this, different frequencies decay at different rates. When the trailer is empty with door closed the frequencies decay very slowly. If the trailer is empty with door open then the sound waves and thus the frequencies can escape through the open door and hence they decay faster compared to the closed door condition. Similar explanation is also applicable to other load and door conditions. This variation in the decay rates of different frequencies for different load and door conditions coupled with the change in the resonant frequency can be utilized to detect unintended load variations. Table 6.1 on page 69 summarizes approximate frequency range and the time taken for the different frequencies to decay for different load conditions. Thus, this report has made an attempt to show that the concept of acoustical signature monitoring (ASM) can be taken a step further to prove that ASM is practically viable. Though road conditions, weather conditions and other unexpected noise influence the echo signal, these noises can be removed using suitable signal processing techniques.

Cases	Duration (sec)	Frequency Range (kHz)
Empty door closed	0.9	1.7 to 6.0
Empty door open	0.55	1.8 to 5.5
One third, door closed	0.4	2.0 to 5.0
One third, door open	0.35	2.0 to 5.0
Two third, door closed	0.30	2.0 to 6.0
Two third, door open	0.25	2.0 to 5.5
Full, door closed	0.20	1.8 to 5.5
Full, door open	0.20	1.7 to 5.0

Table 6.1: Summary of approximate frequency range and decay times for different load and door conditions.

6.4 Future work

As mentioned in the beginning, this report is more about proving a new concept rather than implementing the concept as an application. The results and conclusions shown here are empirical. In order to make this concept practically useful a method has to be evolved so that it can be implemented on a low cost device.

One way of implementing it could be to derive a mathematical equation for the rate of decay of the magnitude of different frequencies. A mathematical relation/equation is relatively easy to implement in a digital signal processor. From this mathematical relation, rates of decay for different conditions can be found and stored as references for comparison. The next step would be to design a system where it will transmit signals every few milliseconds and collect samples of reflected waves and calculate the rate of

decay of the magnitude of different frequencies and compare it with each of the standard rates stored as reference. The standard rate with which the sample has least error will indicate the load status or trailer (or container) condition.

Another way of realizing a system based on ASM is to have an adaptive system. Here the system will take sample echo signals at the beginning for reference and then takes samples every few milliseconds later and compare it with the reference values taken at the beginning. Also such an adaptive system can be designed to adjust itself to different noise conditions and that way we can prevent false alarms from being raised.

The data for this report was conducted in a controlled environment. For this concept to be practically implementable a method has to be evolved to filter out noise due to engine vibrations, different road conditions, weather. The technique of wavelet transforms will be a handy tool in filtering noise, more about this topic can be found in appendix A.

APPENDIX A

A.1 Wavelet transforms

A considerable portion of this section has been referenced from two sources, 'Wavelet Transforms: Introduction to Theory and Application' by R. M. Rao and A. S. Bopardikar [14] and [11]. A Wavelet can be considered as a small wave like function that is time limited and averages to zero. Wavelet transform is a type of transform that can give both time and frequency information. In Wavelet transforms, a time domain signal is split into different frequency bands by passing it through different stages or levels with each level having a high pass and a low pass filters. This breaking up of the time domain signal continues till the signal is split or decomposed to predetermined levels. After the decomposition there will be a set of frequency bands all belonging to the same signal. When these are plotted on a three dimensional graph having time, frequency and amplitude axes, we will get to know what frequencies exist at what time and have what amplitude. However, we will not be able to get exact frequency information and instead we will have information about a band of frequencies and their corresponding time information. This can be reasoned using "Heisenberg's uncertainty principle" which states that the momentum and position of a moving particle (electrons) cannot be known simultaneously, and this principle when applied to Wavelet theory can be restated as, we cannot exactly know what frequency exists at what time instance, but we can only know what frequency bands exist at what time intervals [11].

A.2 Continuous wavelet transform

A Continuous wavelet transform is represented by the equation

$$C(\tau, s) = \int_{-\infty}^{\infty} x(t)\psi(t, \tau, s)dt \quad (\text{A.1}).$$

$C(\tau, s)$ is the Continuous wavelet Transform which is a function of *translation* τ and *scale* s .

$x(t)$ is the time domain signal.

$\psi(t, \tau, s)$ is the wavelet function which in turn is a function of time t , translation τ and scale s .

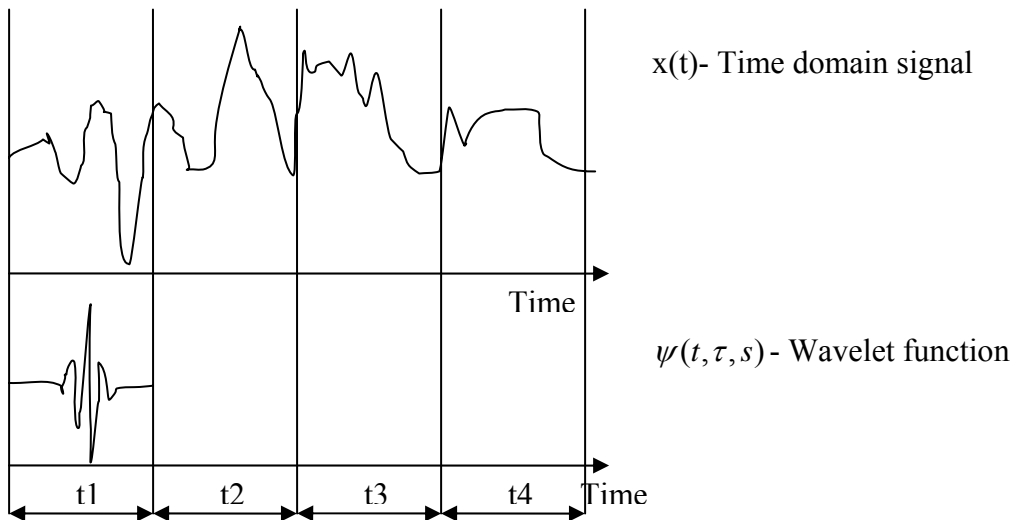


Figure 46: Continuous wavelet transform.

The meaning of the equation A.1 can be explained with the help of Figure 47. The signal $x(t)$ is divided into different time slots t_1 , t_2 , t_3 and t_4 . According to the equation, we assume a value for translation τ , say t_1 and scale s_1 in the wavelet function and as a first step we multiply the signal $x(t)$ and then integrate the product over the entire length of

the signal, let CWT1 be the value of this mathematical step. In the second step the Wavelet function is translated to the second time slot t_2 , i.e. τ now takes the value t_2 . Then the first step is repeated, let the value in this step be CWT2, this process is continued for the entire length of the signal including t_3 and t_4 , let the values in these steps be CWT3 and CWT4.

Next we change the scale s (dilation or compression) to a new value and repeat the above procedure. In the end we will be having numbers CWT $_n$, $n = 1, 2, 3 \dots$ up to a predetermined level. These coefficients are then plotted, with one axis as scale, another as time/translation and the third as amplitude. These numbers give insight into signal frequency and time information.

When the scale is a small number, it means the wavelet is compressed and correlation coefficient will be high for high frequencies in other words small values of scale is good for identifying detailed information in a signal. If the scale is a big number the wavelet is dilated and the correlation coefficient will be high for low frequencies in other words the large values of scale is good for identifying coarse features or approximate information of a signal.

A.3 Discrete wavelet transform

In case of continuous wavelet transform the amount of mathematical calculations for every possible value of scale is very high and to reduce these calculations and improve

the efficiency and utility of wavelet transforms, discrete wavelet transforms are used where the scale and translation values are powers of two just like in case of FFT.

In many practical applications we are mostly interested in the low frequency components than the high frequency components. For example, speech signals. In speech signals if high frequency components are removed the signal will still be good enough to decipher what is being said, but if low frequency components are removed, it is not possible to clearly understand the message. In other words we say that low frequency component of a signal is the *approximation* part of the signal while the high frequency component of the signal is the *detail* part. This also means that high scales are associated with approximations and low scales are associated with details.

A.4 Decomposition filter

The principle on which the discrete wavelet transform works has been explained at the beginning of section A.3, i.e. splitting the signal into different bands by passing it through a series of high pass and low pass filters. One of the applications of this method is in the removal of noise. This can be better explained using an example.

Consider a sinusoidal signal of frequency 10 Hz corrupted by random noise. This is shown in the Figure 48 on page 75.

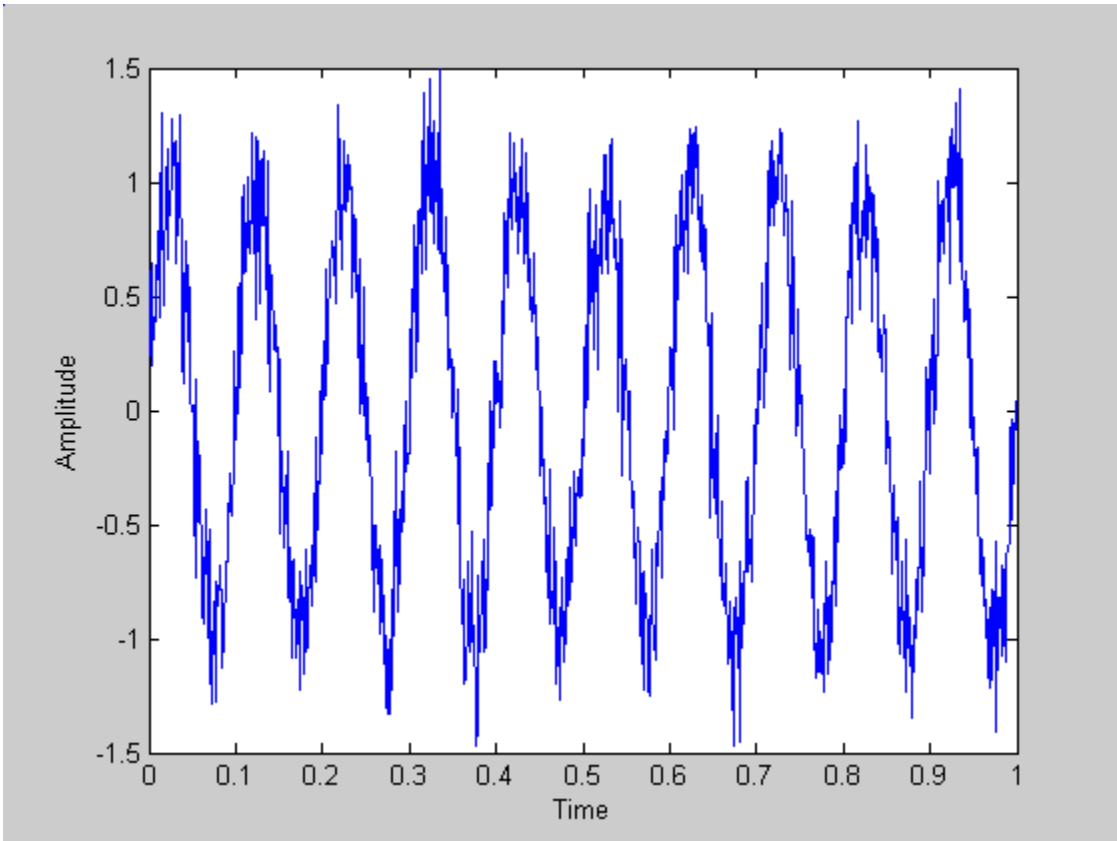


Figure 47: Corrupted sinusoidal signal of frequency 10 Hz.

Let the above signal be represented as

$$x_1(t) = \sin(2\pi 10t) + \text{random noise} \quad (\text{A.2})$$

After passing this signal through first stage of low pass and high pass filters we have two signals (approximation signal, A1 and detail signal, D1) as shown in Figure 49 (page 76).

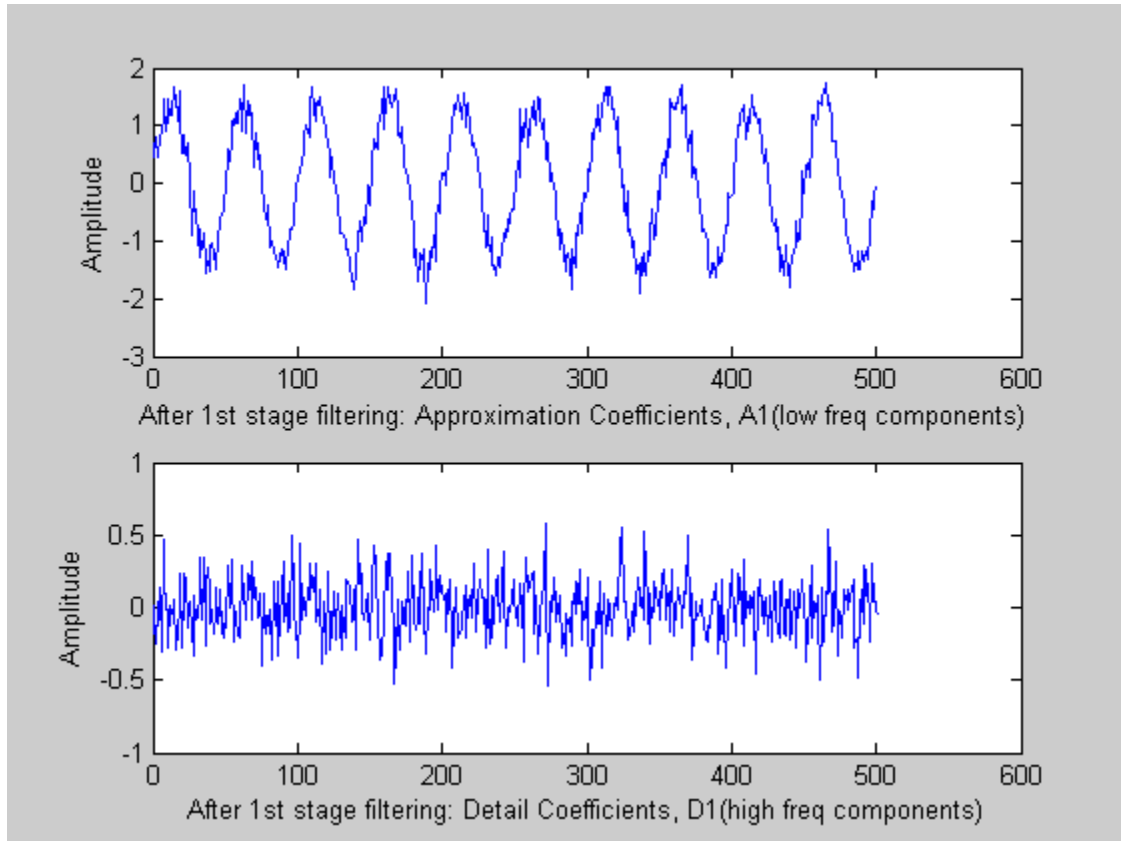


Figure 48: Low frequency and high frequency components after 1st stage filtering.

A1 coefficients are then passed through second stage filtering to get two signals approximation signal, A2 and detail signal D2. In the third stage A2 coefficients are again passed through high pass and low pass filters to further filter out noise. This process of filtering continues till we get satisfactory results. Figure 50 shows the filtering process up to 3rd stage. Close observation shows that in A1 we have half the number of sample points compared to the original signal and A2 has half the number of sample points compared to the A1, and A3 has half the number of sample points compared to A2. This is because of down sampling to avoid unnecessary accumulation of data points.

We can see that after each filtering stage the approximation signal is more refined than the previous stage approximation signal.

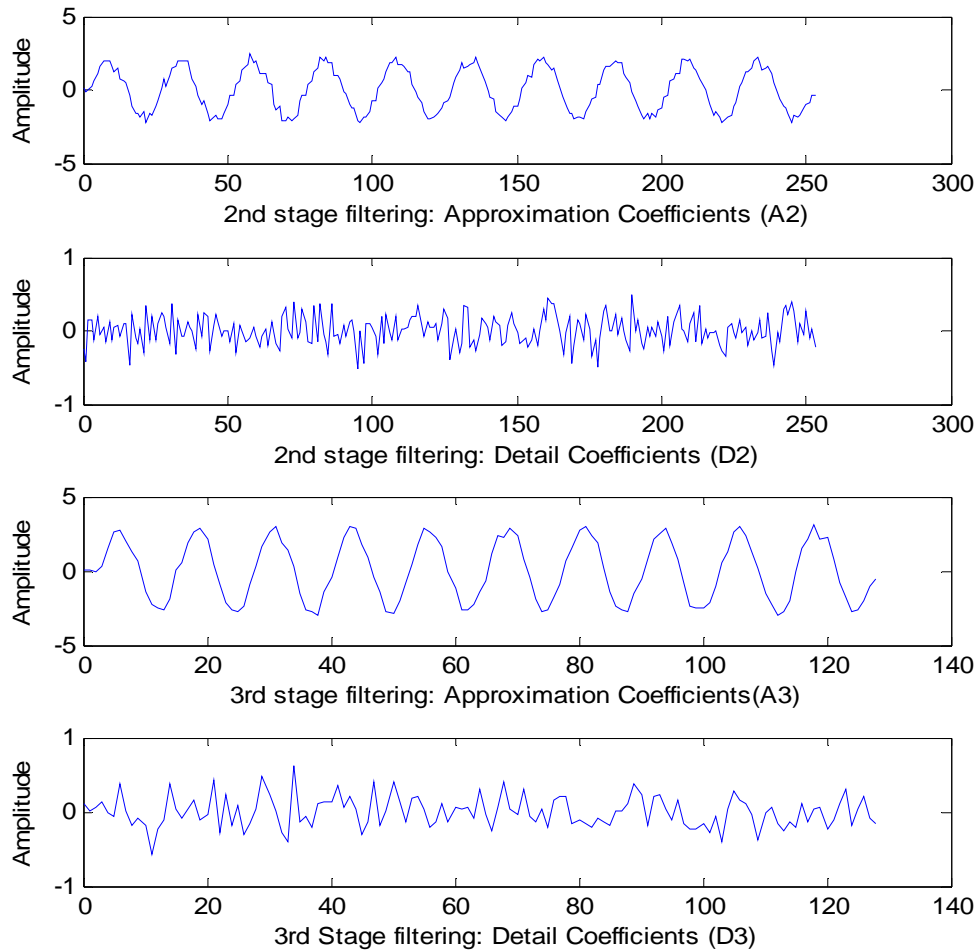


Figure 49: Low and High frequency components after second and third stage filtering.

A.5 Applications of wavelet transform

Wavelet transform has wide area of applications like image compression, detecting breakdown points, de-noising signals, de-noising images, in biology for detection of good cells from bad ones, detecting cracks in metals or characterization of metal surfaces.

Wavelet transforms are also helpful to take this report from concept level to implementation level. The echo inside a trailer/container will be corrupted by noise from different sources like wind, engine, and vibration of the body which in turn depends on the speed of the vehicle and road conditions. The echo signal has to be filtered to remove all the added noise. Wavelet transforms is a helpful mathematical procedure in de-noising a signal.

APPENDIX B

Introduction

Most of the information given in this appendix has been referenced from the books: 'The World of Sound' by Vernon M. Albers [13], 'Our Acoustic Environment' by Fredrick A. White [12], 'Hand Book of Noise Measurement' by Arnold P. G. Peterson and Ervin E. Gross Jr [15].

When sound waves propagate there will be compressions and rarefactions. These compressions and rarefactions are nothing but different levels of sound pressure. The amplitude of sound waves is usually specified in terms of its pressure.

Sections B.1 to B.4 are referenced from 'Over Acoustic Environment' by Fredrick A. White [12].

B.1 Sound pressure

Sound pressure is the variation in the pressure levels from the local ambient pressure caused by a sound wave. The SI unit of measurement of sound pressure is Pascal (the symbol for representing Pascal is 'Pa')

B.2 Sound pressure level (SPL)

Human ear is generally sensitive to sound waves from 20 Hz to 20 kHz. Sound waves beyond 20 kHz are called ultrasonic waves. The sensitivity of human ear to sound waves

varies over a wide range of amplitudes and hence is measured as a level on a logarithmic decibel scale, sound pressure level (SPL), L_p .

Sound pressure level is defined as

$$SPL, L_p = 10 \log_{10} \left(\frac{P^2}{P_0^2} \right) = 20 \log_{10} \left(\frac{P}{P_0} \right)$$

where ' p ' is the root mean square sound pressure and ' p_0 ' is a reference sound pressure.

According to ANSI standard S1.1-1994, the reference sound pressure in air is 20 μ Pa.

The spectral response of human ear is not constant/flat and hence sound pressure levels are often frequency weighted so as to match the measured level with perceived levels. The International Electrotechnical Commission (IEC) has defined several weighting schemes and the A-weighting scheme is a close match with regards to the response of the human ear to noise and A-weighted sound pressure levels are labeled dBA. Similar to A-weighting scheme there are other schemes like B-weighting, C-weighting and D-weighting schemes. Each weighting scheme has a different transfer function that results in different gain curves. Initially A-weighting scheme was used for low level sounds, B and C schemes for louder sounds and D weighting scheme for much louder sounds like aircraft engine.

B.3 Sound power

Sound power is a measure of sound energy per time. If I is the sound intensity and A is the area then, sound power $P_{acoustic} = I A$

The logarithmic measurement is given by

$$L_w = 10 \log_{10} \left(\frac{P_1}{P_0} \right) dB$$

The reference sound power P_0 is normally taken to be 10^{-12} watt

B.4 Sound power level

Sound power level is also measured in terms of logarithmic scale. It is the measure (logarithmic) of sound power in comparison to a specified level. Sound power level is given by the equation

$$L_w = 10 \log_{10} \left(\frac{W_1}{W_0} \right) dB$$

Where W_1 and W_0 are powers in watts. Though sound power level is also measured in terms of dB and its reference unit is watts and the value normally assumed for the reference W_0 is 10^{-12} watt

REFERENCES

- [1] K. Finkenzerler, *RFID Handbook : Radio-Frequency Identification Fundamentals and Applications*, New York: John Wiley 1999
- [2] B. H. Wellenhof, H. Lichtenegger, J. Collins, *Global Positioning System: Theory and Practice*, Wien, New York, NY: Springer-Verlag 1993
- [3] H. Guo, J. A. Crossman, Y. L. Murphey, M. Coleman, "Automotive signal diagnostics using wavelets and machine learning," *IEEE Trans. Vehicular Technology.*, vol. 49, no. 5, pp. 1650-1662, Sep. 2000
- [4] M. J. Dowling, "Application of nonstationary analysis to machinery monitoring," *IEEE International Conf. on Acoustics, Speech and Signal Processing, ICASSP-93.*, vol. 1, pp. 59-62, Apr. 1993
- [5] G. Porges, *Applied Acoustics*, New York: John Wiley 1977
- [6] M. Norton, D. Karczub, *Fundamentals of Noise and Vibration Analysis for Engineers*. New York, NY: Cambridge University Press, 2003
- [7] M. Rettinger, *Acoustic Design and Noise Control*. New York: Chemical Pub. Co., 1977
- [8] R. G. Lyons, *Understanding Digital Signal Processing. 2nd Edition* Indianapolis, In: Prentice Hall PTR 2004
- [9] MATLAB is software for technical computing and Model-Based Design by *The Mathworks, Inc.*, <http://www.mathworks.com/>
- [10] J. Cooley, J. Tukey, "An algorithm for the machine calculation of complex series," *Math. Comput*, vol. 19, no. 90, pp. 297-301, Apr. 1965
- [11] R. Polikar, *Course: 0909.554, Theory and engineering applications of wavelets*, College of Engineering, Rowan University, Spring 2006
- [12] F. A. White, *Our Acoustic Environment*, New York, NY: John Wiley 1975
- [13] V. M. Albers, *The World of Sound*, South Brunswick, NJ: A. S. Barnes 1970
- [14] R. M. Rao, A. S. Bopardikar, *Wavelet Transforms: Introduction to Theory and Application, Har/Dsk Edition*: Prentice Hall PTR 1998

- [15] Arnold P. G. Peterson, Ervin E. Gross Jr, *Hand Book of Noise Measurement*, Concord, MA: General Radio, 1977
- [16] A. V. Oppenheim, A. S. Willsky, S. H. Nawab, *Signals and Systems*, New Delhi, India: Prentice Hall of India Private Limited 2002

